TransFormers
for Extreme Environments

May 2014

Phase I Final Report
by Adrian Stoica,
Michael Ingham,
Leslie Tamppari,
Karl Mitchell, and
Marco Quadrelli

**Final Report
Early Stage Innovation
NASA Innovative Advanced Concepts (NIAC)**

TransFormers for Extreme Environments:
Projecting Favorable Micro-Environments around Robots and Areas of Interest

**Adrian Stoica, Principal Investigator
Co-Investigators: Michael Ingham, Leslie Tamppari, Karl Mitchell,
and Marco Quadrelli**
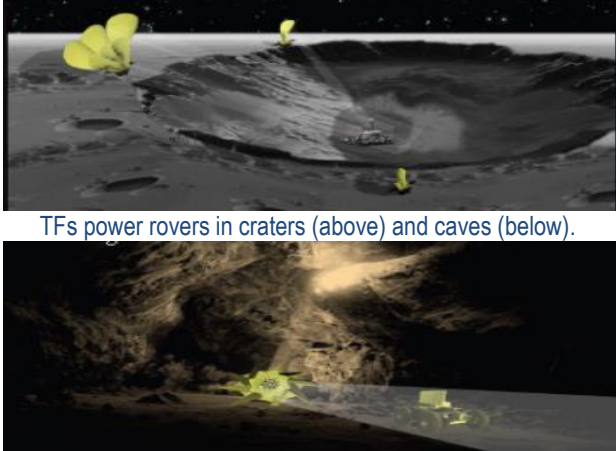
Jet Propulsion Laboratory

May 2014

Acknowledgement

Overview Chart

Concept

"Surviving Extreme Space Environments" (EE) is one of NASA's Space Technology Grand Challenges; we propose a paradigm shift in addressing this challenge. TransFormers (TFs) *transform a <u>region of an extreme environment into a favorable micro-environment</u>*, projecting energy at the precise location where robots or humans operate. TFs often use *shape transformation* to control the energy projection.

TFs power rovers in craters (above) and caves (below).

Mission Scenarios, TF Technologies

Phase I examined the reflection of solar energy into shadowed areas, dark and cold: in the context of missions to craters on the polar regions of the Moon and Mercury (with ice deposits) and caves on the Moon and Mars (interest for their scientific value, as well as for sheltering human bases). TFs project energy to power solar cells, heat, illuminate, and relay communications to a habitat or to rovers down in craters or deep in caves.

Specifically, the scenario for a Lunar South Pole mission at Shackleton crater (20-km diameter) was analyzed in more detail. Placed at a favorable point on the rim (A.2 site), the TF sees 100% of the solar disk 85% of the time, with only 3 days without full Sun. The requirement was to project 300 W/m^2, enough to operate for Mars Science Laboratory (MSL)- or Mars Exploration Rover (MER)- class rovers for long-duration operations at 10 km into the crater. We compared this with the RTG solution, and examined the potential of energy spill to sublimate the volatiles of interest. We sought solutions of TFs that pack within 1 m^3 and weigh less than 100 kg.

Main Findings

- The needed diameter of a TF to power rovers 10 km into Shackleton crater was determined to be 40 m (~1200 m^2), sufficient for MSL-level (~300 W electrical power).
- The component technologies for implementing a 1200-m^2 autonomous TF are at TRL 3 and higher. Integration is between TRL 1 and 2.
- The mass of a radioisotope thermoelectric generator (RTG) prevents its use by an MER or smaller rover. TF cost is projected to be much lower than RTGs (~$45M); multiple rovers and multiple missions require no additional cost.
- Short-term (hours) illumination of regions containing volatiles appears to have no major effects. We discuss alternatives to avoid longer exposures, which need further refinement.
- TFs show considerable advantages for successive/diverse missions in the same region, and for simultaneous powering of multiple platforms, enabling new classes of missions at relatively close, yet, currently inaccessible places of interest.

Recommended Steps

Advance the TF concept in the context of a mission scenario at Shackleton crater, with:

1. <u>Focus on a polar volatile mission</u>—perform a detailed mission concept analysis, eliminate highest remaining risks, increase TRL to 3, providing:
   - Robustness solutions to dust, radiation, and meteorites;
   - Option of multi-hop reflections to project beyond line of sight, helping controlled energy focus to reduce spill—**key for missions into caves;**
   - Design study targeting a scalable TF unit of 1000 m^2 with a 100-micron layer (0.1 m^3) and a weight of 10 kg

2. <u>Tap into the potential of new classes of missions</u>
   - Simultaneous powering/warming of multiple robots for effective mining, construction, and large-scale exploration;
   - Covering a large region, for a lunar base
   - A permanent multi-mission resource in the polar area of value to NASA and its partners.

Executive Summary: Main Findings and Recommendations

"Surviving Extreme Space Environments" (EE) is one of NASA's Space Technology Grand Challenges. Power generation and thermal control are the key survival ingredients that allow a robotic explorer to cope with the EE using resources available to it, for example, by harvesting the local solar energy or utilizing the onboard radioisotope thermoelectric generator (RTG). A new, complementary perspective, the objective of this study, is to project energy to change the EE in the precise local area around robotic or human explorers, transforming it into a favorable/survivable micro-environment (FME).

The micro-environment projection would be done by 'TransFormers' (TF), thus named because of two key properties: they transform the environment, and they adapt to needs through shape and functional transformation. TFs are a class of robotic systems. Their surface embeds (a) reflectors to redirect energy, (b) solar cells and batteries to retain power for its own operation, (c) actuation and control elements to change the shape and to precisely redirect energy, and (d) computing.

The primary benefit of a TF is to make possible affordable missions that require survival for long periods of time without direct or with limited solar input. This way, environments without sunlight (such as craters and caves) can use TFs located in Sun-illuminated areas outside to project energy inside the permanently shaded areas, power solar panels, heat, illuminate, and relay communications. This report shows how a TF can be used in missions to lunar craters, lunar lava tubes, and martian caves, relevant both for space science and for human exploration, as well as missions to Mercury polar craters. TFs are the preferred solution for some missions and the enabling solution for new mission categories, in particular missions with multiple smaller rovers/probes, which cannot accommodate their own power/heating in the constrained size.

We performed a high-level comparative assessment for crater missions on the Moon and Mercury, as well as lava tubes/caves on the Moon and Mars. For a mission deep inside the Moon's Shackleton crater, we performed a more detailed analysis, looking at mission trade-offs, and optical and thermal analyses for providing sufficient power for charging the solar panels and maintaining the rover warm while working at the 40–70K crater temperatures. We conducted these analyses for three classes of rovers, the sizes of the three generations of Mars rovers: the Sojourner Rover, Mars Exploration Rover (MER), and the Mars Science Laboratory (MSL) Rover. A rover with MSL technology is able to satisfy the full set of target scientific exploration requirements with 300 W of power. An MSL-sized rover would carry a sampling arm and a drill; a mass spectrometer for detecting ice, chemicals, and carbon; an X-ray diffraction (XRD) for mineralogy; and a ground-penetrating radar (GPR) for subsurface structures. This allows for a full geological and mineralogical exploration and for ice/mineral sampling, as well as for subsurface structure analysis. A capable cave exploration mission might require a stereo camera, a spectrometer for ice/mineral detection, an ultraviolet (UV) fluorescence instrument for organics detection, a seismometer for interior structure, a GPR for assessing cave stability, a sampling arm, and a mass spectrometer for carbon detection.

The TF solution has been found sufficient to power rovers such as described above. Some of robotic missions described can be done using RTGs, yet TF has advantages over an RTG solution in several situations, for example: use of smaller robots; lower cost missions (Discovery-size), with increasing cost benefits for repeated missions in the same area; and powering/warming multiple rovers/vehicles. It is also a more desirable solution for human operations on the Moon.

We performed calculations for the needed TF area to project solar power to 10 km into Shackleton crater (20-km diameter). We did a preliminary evaluation on the effect of solar illumination in causing ice sublimation. We explored means to reduce/limit the spill of energy

around the rover so it does not heat and sublimate the ice (the RTG also must eliminate almost 2 kW of thermal power).

We also looked at the needed functions and the ability to embed those functions in ~100-micron layers, to be integrated such that the weight is below 100 kg and packs in less than 1 m^3. We considered built-in functions including pointing, Sun tracking, and a means to compute and actuate to the needed shape. The designs examined require compact packing and light weight for the flight to the Moon and the surface transport by the rover to the rim.

The study eliminates the identified risks and formulates a new set of challenges that appear in the advancement of the concept. We propose to address them in a NIAC Phase II study.

Main Findings

- In short term, the highest return on investment for science and in preparation of manned missions comes from a TF mission at the Lunar South Pole.
- A 40-m diameter (~1200 m^2 surface) TF is needed to project 300 W/m^2 10 km into Shackleton crater sufficient for MSL level (~300 W on 6-m^2 solar panels).
- A 10-m-diameter TF is able to provide nearly full solar irradiation up to 1 km distance. This supports affordable exploration of lava tubes and would support a permanent base—projecting sunlight inside caves would require multiple reflections, beyond the line of sight (BLOS) of the TF on the skylight. This needs further study.
- The component technologies for implementing a 1200-m^2 autonomous TF are at TRL 3 and higher. Integration is between TRL 1 and 2.
- A 1200-m^2 surface could be packed within 1 m^3, and could weigh less than 100 kg. The study offers promise that needed functionality can be packed in the 100-micron layer, and large surfaces can be compactly packed and unpacked, for example, in origami style.
- The RTG mass prevents its use by MER or smaller rovers. TF cost is projected to be much lower than RTGs (~$45M); multiple rovers and multiple missions require no additional cost.
- Short-term (hours) illumination of regions containing volatiles appears to have no major effects. We discuss alternatives to avoid longer exposures, which need further refinement.
- TFs show considerable advantages for successive/diverse missions in the same region, and for simultaneous powering of multiple platforms, enabling new classes of missions at relatively close, yet now inaccessible places of interest.

Recommendation

Advance the TF concept in the context of a mission scenario at Shackleton crater, with:

1. **Focus on a polar volatiles mission**—with a detailed mission concept analysis, eliminate highest remaining risks, increase TRL to 3, providing:
   - Robustness solutions to dust, radiation and meteorites;
   - Option of multi-hop reflections to project beyond line of sight, **helping to control the focus of power and hence reduce the influence on the explored area;**
   - Design study targeting a scalable TF unit of 1000 m^2 with a 100-micron (0.1 m^3) layer and a weight of 10 kg

2. **Tap into the potential of new classes of missions**
   - Simultaneous powering/warming of multiple robots for effective mining, construction, and large-scale exploration; large area projection for a lunar base
   - A permanent multi-mission resource in the polar area of value to NASA and its partners.

Contents

List of Figures

List of Tables

1   Introduction

1.1   The Need to Survive Extreme Space Environments (EE)

Imagine that we could remotely control the environment surrounding the vehicles adventuring in unexplored areas of the Solar System, such as the dark interiors of permanently shadowed craters or the depths of caves on the Moon, Mars, or Mercury (**Figure 1.1**). These places are very valuable, since they often harbor ice water; may hide possible traces of life or preserved vestiges of the past, shielded from the surface influences; and because they offer protective habitats for future human missions. Yet, they are dark and cold, and hard for robots and humans to survive in.

Addressing extreme planetary environments is one of the main challenges of space in-situ space exploration, both robotic and human. Temperature, radiation, and other factors make the missions inconceivable at present. Providing remotely controlled protection to the in-situ explorers of EE, *projecting and controlling an ameliorated micro-environment* around them, is a new idea, with *potential broad implications for both robotic and future human spaceflight.* EE may be characterized by low or high temperatures, high radiation, high pressure, etc. The new concept discussed here directly addresses the "Surviving Extreme Space Environments Challenge," one of the NASA's Space Technology Grand Challenges [NASA GC], specifically aimed at enabling robotic operations and survival, in the most extreme environments of our Solar System.
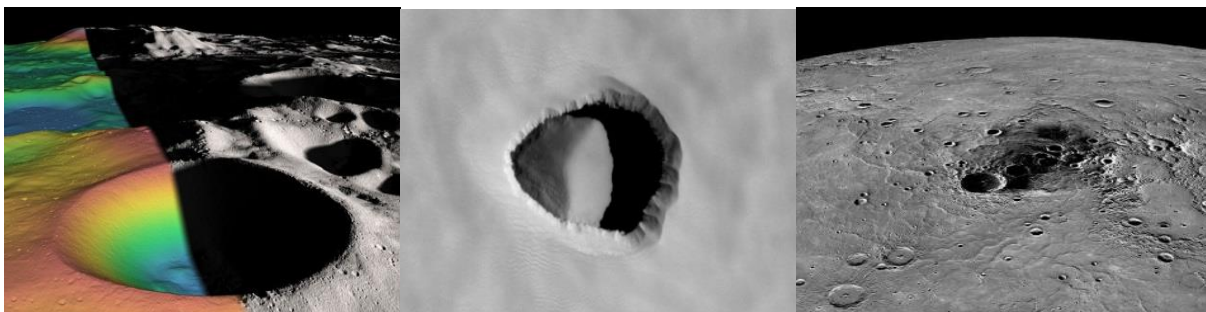
Figure 1.1. Science targets—permanently shaded craters and caves on the Moon (Shackleton crater, candidate for lunar outpost- synthetic image, left), Mars (cave skylight near Arsia Mons, center), and Mercury (ice-harboring craters near North Pole, right). Credit NASA.

1.2   Inducing Favorable Micro-Environments within EE

Inducing a favorable micro-environment within an EE is a new paradigm. TransFormers (TF) **remotely project and control a favorable local micro-environment (around rovers/habitats)** where exploration, exploitation, or human visits will take place. TFs **transform the environment, and to do so often perform a shape transformation**. Their body surface embeds reflectors and solar cells; they would also include antenna elements for communication, and actuation and control elements for shape change. TFs are a new class of robotic space systems for controlled projection of needed resources/energy.

TFs may totally transform the way NASA performs missions in EE. Built of light, thin surfaces, they would pack in compact volumes, making them affordable cargo. At destination, the TFs would deploy to large surfaces, directing energy to the precise area where needed, up to many kilometers away. The current space exploration model relies on the explorer carrying energy sources (e.g., RTG) or producing energy in situ, from local resources; TFs add a new

modality—the remote projection of resources/energy where needed, when needed. Current solutions use local resources (on platform energy generation/conservation)—cope with the environment. TFs add a new, complementary perspective: remote resources are projected to induce a survivable micro-environment—they change the environment (locally).

1.3   Projecting Solar Energy

TFs are a generic concept, independent of the form of resource provided to create a favorable locale. The Phase I scope was limited to TF supporting rover missions to *cold, dark sites* on planets/bodies with *thin or no atmospheres*. These are conditions characteristic of the polar craters on the Moon/Mercury and caves on the Moon/Mars (high-priority exploration sites) posing formidable challenges to current technologies in terms of maintaining thermal and power regimes, and coping with unknown hazards generally not discernible with Earth-based radar scans or orbital imagery.

This study focuses on the use of solar energy to provide FME in the cold dark sites; this section provides a background on solar irradiance as well as other environmental characteristics.

Figure 1.2 shows the sun radiation intensity at the surface of the Sun and at distance D from the Sun. The total solar radiation emitted by the Sun is given by the power density, σT^4 (T=5778K), multiplied by the surface area of the Sun ($4\pi R^2_{sun}$), where R_{sun} is the radius of the Sun. The surface area over which the power from the Sun falls at distance D from the Sun is $4\pi D^2$. The solar radiation intensity, H_0 in (W/m^2), incident on an object, is $H_0=(R^2_{sun}/D^2) \times H_{sun}$,
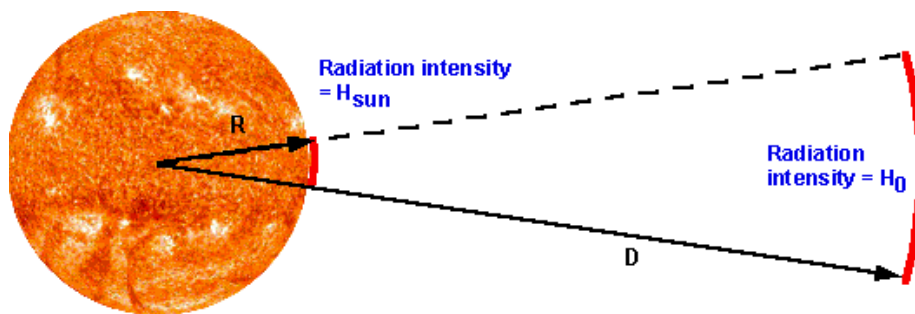
Figure 1.2. Solar radiation intensity at a distance D.

Source: http://www.pveducation.org/pvcdrom/properties-of-sunlight/solar-radiation-in-space

where: H_{sun} is the power density at the Sun's surface (in W/m^2), as determined by Stefan-Boltzmann's black body equation; R_{sun} is the radius of the Sun in meters. **Table 1.1** summaries some environmental characteristics on the inner planets including the solar irradiation intensity.

Table 1.1. Some environmental characteristics on Mercury, Venus, the Moon, and Mars.

Planet (Moon)	Distance (×10⁹ m)	Mean Solar Irradiance (W/m²)	Temp (min/mean/max)	Gravity m/s²	Atmospheric density (kg/m³)	Dust	Winds	Axial Tilt
Mercury	57	9116.4	590-725K	3.7	Vacuum	-	-	2.11°
Venus	108	2611.0	460C	8.87	65	Trace	Slow	
Moon - Polar	150	1366.1	70K/130K/230K	1.62	3×10^{-15} atm (0.3 nPa)	Yes	No	1.54°
Mars	227	588.6	120K-300K	3.71	0.0155	Significant	Strong	25.19

SOURCE: http://quest.nasa.gov/aero/planetary/mars.html

As a comparison, the mean solar radiation at Jupiter (as indicative of Europa) at 778×10^9 m distance from the Sun is 50.5 W/m^2, while at Saturn (as indicative of Titan) at 1426×10^9 m is

15W/m^2. TFs would also work on remote outer planets. However, at low solar intensity, much larger surfaces would be needed for using solar energy. A different energy source may be more efficient.

1.4 Sunlight Reflection Creating Micro-Environments on Earth

Bringing sunlight to target areas has already been tried on Earth. The following two examples illustrate the use of the concept and the derived benefits.

Heliostats Reflecting Sunlight into Valleys Below

To see the Sun during winter months, heliostat mirrors have been built to reflect the sunlight into deep valleys where towns are situated. The towns of Rjukan (Norway) and Viganella (Italy) are both situated in deep valleys where mountains block the Sun's rays for months. The two towns have built computer-controlled mirrors that track the Sun and reflect sunlight downwards. The Rjukan mirror reflects a 600-square-meter beam of sunshine into the town square below, as seen in **Figure 1.3**.

Figure 1.3. Heliostats illuminating towns in deep valleys: Rjukan (Norway) and Viganella (Italy).
SOURCE: http://sourceable.net/century-old-engineering-idea-brings-sun-to-mountain-town

Mirrors Reflecting Sunlight into Tunnels

It is said that in ancient Egypt, mirrors were used to illuminate tunnels being dug, and while there is no strong evidence for that, presently, guides at historic Egyptian sites use mirrors to reflect light inside the tunnels to let tourists see inside. Yet, the method has clearly been used in the past—we have evidence that in 1890, the Union Oil Company dug a 1,940-foot tunnel into the base of Sulphur Mountain. Engineers used mirrors to reflect sunlight into this tunnel for lighting and alignment, as illustrated in **Figure 1.4**.
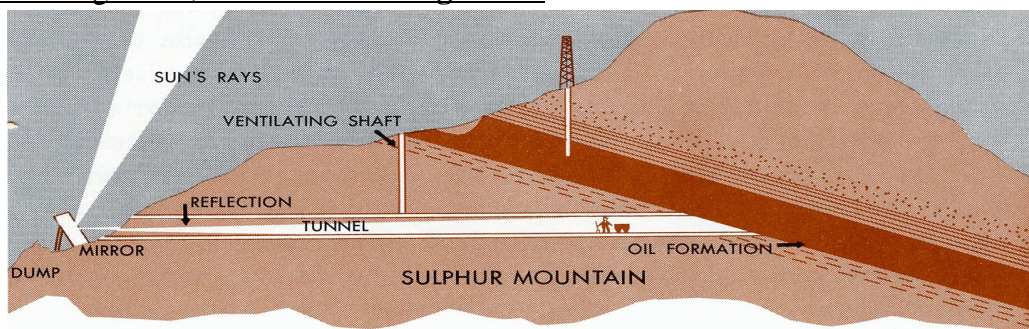
Figure 1.4. Mirrors reflecting sunlight into tunnels

SOURCE: http://www.theatlantic.com/infocus/2013/10/using-giant-mirrors-to-light-up-dark-valleys/100613

The TFs we will analyze are more complicated than Rjukan heliostats—they need to track a moving rover (not only the Sun), be light weight, and pack in a compacted folded volume—yet, the essence of the idea is the same.

1.5   Benefits of Studying TFs

The study of TFs is beneficial from a multitude of perspectives:

- TFs offer a <u>new paradigm for survivability in EE.</u> The study will show major implications, most importantly the enabling of missions with multiple smaller rovers (which cannot afford their own heating/power) and a source for permanent power for continuous presence over multiple missions.

- The TF concept opens *new frontiers of exploration and scientific discovery in relatively close*, yet hard-to-reach destinations.

- Forwards *solar concentration* as a promising area for DOE applications.

- From a <u>robotic control</u> perspective, advances state of the art in *controlled projection of sunlight on a moving target*.

- Progress in *shape-changing techniques* advances field of *soft robotics* and origami robotics, paving way to highly <u>reconfigurable robots</u>.

- From <u>materials and embedded electronics</u> perspective, *integrated TF-fabric* represents advancement over electronic fabrics (E-fabric), extending the applications, e.g., to smart homes/environments.

- From <u>systems</u> perspective, performs feasibility assessment of *innovative multifunctional system* integrating embedded materials, distributed sensing and actuation, and shape change.

1.6   Phase I Objectives and How These Were Met

Phase I of the NIAC task entitled, "Transformers for Extreme Environments", investigated the requirements for TF, viability of TF, and technologies for creating TF. It explored mission concepts that could be enhanced or enabled with TF technology.

The study had two objectives. The **first objective** was to perform an analysis and determine, in the context of mission scenarios of robotic exploration of permanently shadowed polar craters (for the Moon and Mercury) and caves (for Moon and Mars), *what requirements TF needs to satisfy*, and *what measurable benefits can TF bring to the missions*. An important result obtained is the relationship between TF size and the distance to which a desired level of solar power can be transmitted on the Moon. Other important results relate to the needed surface quality of the reflector, pointing accuracy, and to the degree to which there is a wider distribution ('spill') at high distances. In correlation to specific missions, one can determine design specifications for the TF; the study looked at powering Sojourner-, MER-, and MSL-size rovers in caves and crater scenarios, determining the benefits it would bring—the more refined case being an MSL-level mission to Shackleton crater. The study determined that for projecting 300 W/m^2 at 10 km into the crater, a 40-m-diameter TF reflector on the rim is needed (at a very conservative 16% conversion efficiency the rover would need a 6 m^2 solar array, with a more realistic 26%, as it was in fact in MSL, a solar array proposal would compensate for imperfect reflection, angles of incidence, etc.).

The **second objective** was to refine the concept of TF that remotely creates and controls a micro-environment within an extreme environment, *eliminating the main risks to the feasibility of implementing TF*. The study looked at a variety of implementation options for the needed

subsystems, all of which were implemented in less than 100 microns, many in less than 20 microns. A variety of deployment solutions were examined, in particular various forms of origami-based folding, such as, for example, the Miura-ori. Preliminary calculations indicate that the 1000-m^2 TF surface can fit in a 0.1 m^3 volume. This volume, which is equivalent of 100 cubesats, would pack 100/6 Lunar Flashlight mission 6U cubesats, each of 80-m^2 solar sail, and the spacecraft avionics, thus more than 1200 m^2 TF in cubesat technology.

1.7   Organization of the Report

This final report contains the analysis and findings of Phase I organized into four sections.

Section 2 presents the context of several mission scenarios that would become possible through the use of TF. It starts with the science and exploration drivers, the analysis factors and the design questions that were to be answered. A preliminary analysis is performed for four mission scenarios, analyzed at high level, two for craters (the Moon and Mercury) and two for caves (the Moon and Mars) to narrow down on a mission to analyze in more detail and determine a set of high-level requirements for TF.

Section 3 contains a more detailed analysis performed on a mission to Shackleton crater. Here, we performed mission trades, an optical analysis, a thermal analysis, and a preliminary pointing and control analysis to determine design requirements for TF, and eliminate the main risks of the concept; a discussion of the scientific value offered by TF-powered missions of various class TFs is also discussed.

Section 4 contains a high-level feasibility analysis giving examples of state-of-the-art component technologies that could be used to build a TF that would meet the requirements determined in Section 3.

Section 5 makes a summary of what has been done, what it means in the context of expected technology advancements, the potential risks and challenges associated with TF technology, and what remains to be done to mature the concept towards enabling new missions.

2 Space Mission Scenarios

2.1 Science and Exploration Drivers

2.1.1 Polar Craters on the Moon and Mercury

The discovery of ice deposits in permanently shadowed craters of Mercury [1–3] and the Moon [4] presents potential as a resource for both robotic and human spaceflight, but also a big challenge to mission planners. Such ice deposits preserve a unique record of the geology and environment of their hosts, both in terms of impact history (and possibly volcanic activity, if sufficiently ancient) and the supply of volatile compounds (mostly water), and so are of immense scientific interest. To date, these have only been studied indirectly (via remote analysis of impact ejecta) and by remote active radar, but not in a manner that constrains reliably the depths of the deposits, their purity, or the structures within them.

A recently approved mission, the Lunar Flashlight mission, is extremely relevant for this study. Its objective is to project sunlight into a permanently shadowed lunar crater—to do so it uses the reflection from its solar sail, which at launch is packed in a 6-U cubesat (1U = $10\times10\times11$ cm), and then unfolds itself to a 80 m^2 surface, which acts as reflector. In many respects, this is a precursor of a TF.
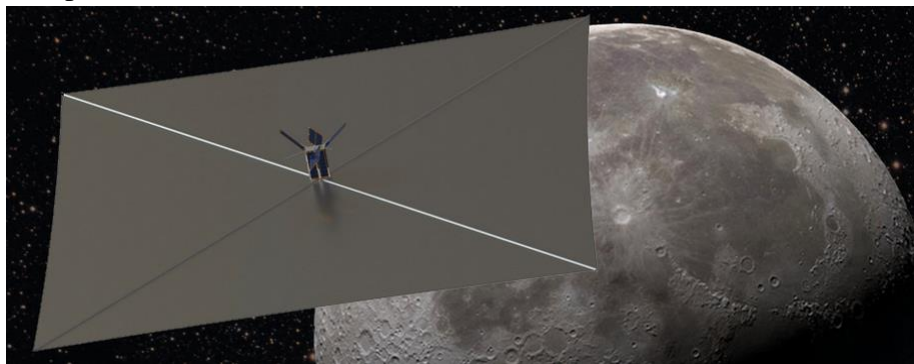
Figure 2.1. Lunar Flashlight solar sail reflecting sunlight into a shaded crater on the Moon.

Image credits: NASA Source: http://sservi.nasa.gov/articles/lunar-flashlight/.

Locating ice deposits in the Moon's permanently shadowed craters addresses one of NASA's Strategic Knowledge Gaps (SKGs) to detect composition, quantity, distribution, form of water/H species, and other volatiles associated with lunar cold traps. The scientific and economic importance of lunar volatiles extends far beyond the question, "Is there water on the Moon?" Volatile materials including water come from sources central to NASA's strategic plans, including comets, asteroids, interplanetary dust particles, interstellar molecular clouds, solar wind, and lunar volcanic and radiogenic gases. The volatile inventory, distribution, and state (bound or free, evenly distributed or blocky, on the surface or at depth, etc.) are crucial for understanding how these molecules interact with the lunar surface, and for utilization potential. Polar volatile data collected by the Lunar Flashlight could then ensure that targets for more expensive lander- and rover-borne measurements would include volatiles in sufficient quantity and near enough to the surface to be operationally useful (http://sservi.nasa.gov/articles/lunar-flashlight/). In many ways, the Lunar Flashlight is a precursor for the lunar missions analyzed later in this study.

2.1.2 Planetary Caves

Terrestrial caves host micro-environments on Earth, with unique and diverse biological communities. Although their presence was first inferred on the Moon long ago (e.g., [Oberbeck], it is the recent discoveries of caves skylights on Mars [5, 6] and the Moon [7] that have stimulated the interest in making them targets for future missions. Such caves are of intrinsic interest as a geologic phenomenon [Boston], provide windows into subsurface geology unaltered by weather (environmental or space), and act as protected repositories for non-speleogenic data including climate, volatile emplacement history, and paleoseismology. They may be the most viable habitats on Mars for endemic life [8], if present, as well as a protective environment for fossils. **Figure 2.1** shows images of lunar and martian caves.
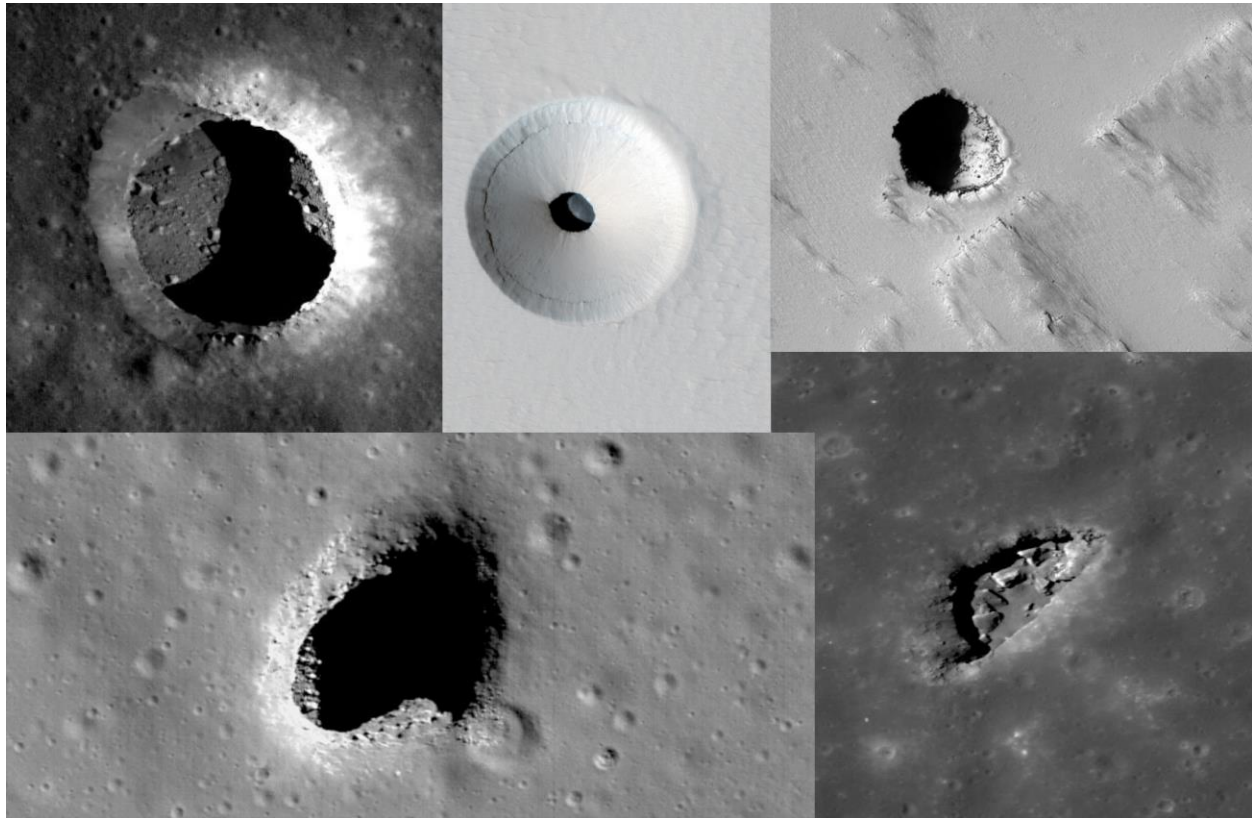
Figure 2.2. A montage of lunar (top-left, bottom-left, bottom-right) and martian (top-center, top-left) pits interpreted as lava tube (cave) skylights, each with scale of 10 s to ~100 m in diameter.

Image credits: NASA/Univ. Arizona/Lunar Reconnaissance Orbiter/Mars Reconnaissance Orbiter.

Lunar caves, and to a lesser extent martian caves, are also of particular interest in manned exploration (Boston et al. 2003). Even more so, that in lunar permanently shadowed craters, they protect astronauts from radiation and space weather (both solar and cosmic), minimizing dosage. However, their temperatures are significantly greater, potentially ~253K (-20ºC) near the equator, compared with, e.g., ~88 K (average), possibly less, on the floor of Shackleton crater, greatly reducing thermal power needs for modules, robots, and space suits. Compared with the insolated martian or lunar surface, they are also far more thermally stable, making thermal design much simpler. They do, however, present greater challenges in terms of mobility and access, and the presence of icy resources is less certain.

2.2   Mission Concepts—Analysis Factors

The mission concepts are driven by the science/exploration goals and benefits.

For craters, the investigations of particular interest include (i) the amount of water they contain and its accessibility for both scientific research and potential use as a resource for human exploration/habitation, and (ii) the nature and amount of organics contained in water deposits that will provide insight into the formation and history of our Solar System.

For caves, investigations of particular interest include (i) the formation mechanisms of caves (speleogenesis) [26]; (ii) the previous planetary conditions (sedimentation, climatology, hydrology, volcanology, etc.) preserved in the caves; (iii) the potential role of caves as habitats for extraterrestrial life (astrobiology) or time capsules preserving life remains and geochemical traces (biosignatures); and (iv) the possibility of cave use for future human exploration purposes.

For each mission concept scenario, it is relevant to:
(0)   Decide on specific scientific investigation and validate the proposed concept;
(i)   Document known crater/cave characteristics;
(ii)   Describe the scientific and exploration targets and formulate related questions;
(iii)   Articulate a set of candidate, known methods for evaluating scientific/resource questions (e.g., possible instruments);
(iv)   Define environmental requirements that TFs will have to account for, including sunlight availability (W/m^2, amount of direct light available throughout the mission) and temperature conditions (min, max T as a function of location in/near crater/cave);
(v)   Define the requirements resulting from the science/exploration scenario goals (power/energy needs for mobility, sampling, and operating instruments; lighting; thermal);
(vi)   Assess current typical rover design capabilities for similar environments and scenarios (e.g., thermal environment for electronics and instruments, power/energy usage of rover/instruments);
(vii) Perform "gap" analysis between current capabilities and mission concept needs, leading to the requirements for TF to "fill the gap".

This section elicits only the minimum level of detail needed to produce a high-level, yet, multi-scenario set of requirements for the TF. More trade-offs including landing conditions are addressed in the refined mission Shackleton crater scenario described in Section 3.

2.3   Risks to be Addressed—Design Questions

The following important question relates to the main risks of the TF concept:

Is it feasible/realistic to project at sufficient distance to make crater and cave missions possible?

More specific questions are:
1. Can sufficient reflected solar power be provided to a rover to power its operation?
2. How big a reflective surface is needed to provide this much light?
3. Can the light be redirected with sufficient accuracy to track the rover at the required distances?
4. How does the TF solution compare with nuclear power provided by MMRTGs—are there relative benefits of using TransFormer(s) to provide this power vs. MMRTG(s)?

5. As the size of the rover decreases, the feasibility of using MMRTGs decreases—can the TF enable a significantly smaller and less expensive mission than is possible with MMRTG?
6. Can it be packaged compactly enough to meet volume constraints ~m^3?
7. Can this size of reflector satisfy constraints on mass (an order of 100 kg was taken for discussion)?

2.3.1 Key TF Design Parameters

Constraints that are relevant and will be assumed or calculated:
- Power needed by an Exploration Rover (ER)
- Illumination needed by ER
- Limit on launch and delivery capability to lunar surface
- Minimum requirements of science payload (power, mass, volume)
- Minimum requirements of communications relay package (power, mass, volume)

The following parameters will be looked at
- TF size
- Distance to rover
- Solar panel size
- Reflectivity of TF surface

The following factors will also be examined
- TF shape
- Number of TF used for mission
- Power needed by TF change its configuration and/or re-point
- Sensors, actuators, and pointing control performance for TF

2.4 Preliminary Analysis for Four Mission Scenarios

2.4.1 Lunar South Pole Crater

Scenario: ER+TF land near a polar crater on the Moon. ER carries compactly packed TF to a predetermined favorable position on the rim; TF unfolds reflecting sunlight to characterize/map the crater before ER goes in; it determines/plans a safe traverse path for the ER. Solarly charged, heliostat, autonomous with supervisory control from Earth; the TF deploys the surface needed and changes shape/orientation as heliostat/rover tracker projects needed resources to the rover. The rover reaches regions of below 100K, where the power projected by the TF is mission-enabling. TF points the reflected energy into ER solar arrays, controls spots of light for the ER to examine its surroundings and to take measurements; also acting as a communication relay to a an orbiter or a surface relay on Malapert or Leibnitz Mountain, with permanent direct view to Earth.
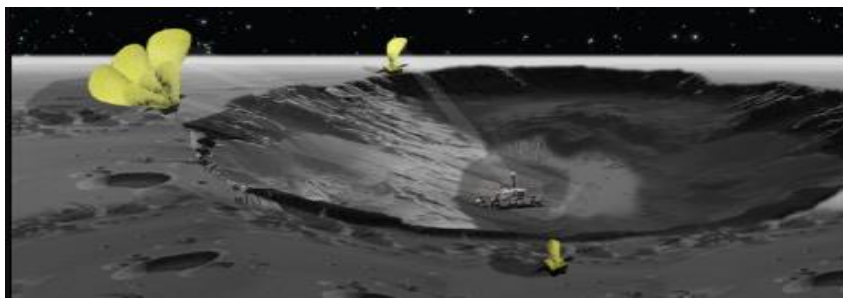
Figure 2.3. Lunar South Pole crater: TransFormers on the rim, projecting a favorable micro-environment to the rover (artist's view).

Scientific investigation: Lunar polar volatiles, ice, and minerals

Locale characteristics (Shackleton crater and similar): Circular crater, 20-km diameter, sunny on the rim ~90% of time, large parts of interior are permanently shadowed; slopes around 30° degrees; hazards; size/location of areas of interest: arbitrary choice in the center of the crater, 10 km from the rim (in fact the center has a mound about 200 m high and may or may not a good target); location of material of interest: subsurface.

Scientific and exploration targets: Full geological and mineralogical exploration. Ice/mineral sampling and analysis. Subsurface structure. The depths of the deposits, their purity, or the structures within them.

Candidate known methods/instruments for evaluating resource questions: Stereo camera for geological analysis and traverse. Spectrometer for ice/mineral detection. Sampling arm/drill to reach subsurface. Mass spectrometer for ice, chemical, carbon detection. XRD for mineralogy; GPR for subsurface structure.

Environmental requirements the TF will have to account for: *Sunlight availability*, amount of direct light available throughout the mission: ~1366 W/m^2, Sun between -2 to 2 degrees above horizon, yet the over 500 m altitude of the rim and the South Pole location allows the Sun to be seen 90% of the time. *Temperature conditions:* 170–230K and above on the rim, 40–70K inside.

Requirements from the scenario goals: Power/energy needs for mobility, sampling, instruments, lighting: 300 W; thermal: 15 W to compensate for heat loss if insulated.

Current rover design capabilities for similar environments/scenarios: Warm box, low-temperature sensor/actuators—power/used of rover/instruments: ~300 W. No solutions for solar power; RTG is the only proven alternative; it needs to eliminate almost 2 kW of thermal energy.

"Gap" analysis: Low-cost mission without RTG requires solar; TF could fill the gap if providing 300 W at 10 km.

2.4.2   Crater on the Mercury North Pole

Scenario: ER+TF land near a polar crater on Mercury. ER carries compactly packed TF to a predetermined favorable position on the rim; TF unfolds, reflects sunlight to characterize/map the crater before ER goes in; it determines/plans a safe traverse path for the ER. Solar powered, the TF is autonomous, changing shape/orientation as heliostat/rover tracker projects needed resources to the rover. The rover reaches regions of below 100K, where the power projected by the TF is mission-enabling. TF points the reflected energy into ER solar arrays, controls spots of light for the ER to examine its surroundings, and acts as a communication relay to a an orbiter.

Figure 2.4. Mercury North Pole and craters containing water ice.

Leftmost: Craters on the Mercury North Pole, Tolkien is 50 km diameter, Prokofiev is 112 km diameter.

Credit: NASA/Johns Hopkins University Applied Physics Laboratory/Carnegie Institution of Washington. Center: Corresponding region in Arecibo radar image, bring areas believed to contain deposits with near-surface water ice. Credit: National Astronomy and Ionosphere Center, Arecibo Observatory. Right-most: TF reflecting into crater.

Scientific investigation: Mercury polar volatiles

Locale characteristics: (North Pole, Tolkien Crater at 88.8N, 149.3E diameter 50 km, also small craters nearby); crater shape: circular; size: 20–50 km; lighting: sunny ~550K on the rim, interior permanently shadowed; size/location of areas of interest: a few km from the rim; depth to material of interest: assumed 0.1–1m.

Scientific and exploration targets: Near surface water ice. The depths of the deposits purity.

Candidate known methods/ instruments for evaluating resource: Stereo camera for geological analysis and traverse. Sampling arm/drill to reach subsurface. Spectrometer for ice.

Environmental requirements the TF will have to account for: *Sunlight availability,* amount of direct light available throughout the mission*: 9116.4 W/m^2, center of the solar disk of the Sun just above the horizon; gravity: 0.38 g. *Temperature conditions:* 550K and above on the rim, 350–80K inside.

Requirements from the scenario goals: Power/energy needs for mobility, sampling, instruments, lighting: 100–300 W; thermal: 15 W to compensate for heat loss if insulated.

Current rover design capabilities for similar environments/scenarios: Warm box, low-temperature sensor/actuators—power/ energy usage of rover/instruments: ~300 W. RTG is the only proven alternative; it needs to eliminate almost 2 kW of thermal energy.

"Gap" analysis: Low-cost mission without RTG requires solar; TF could fill the gap if providing ~300 W/m^2 at 10–20 km.

2.4.3 Cave on the Moon

Scenario: The hollow structure created by ancient volcanic lava flows on the Moon may provide lunar explorers a natural shelter from radiation storms and extreme variations between day and night temperatures encountered on the lunar surface. The images show two narrow trench-like structures, separated by unmodified terrain, interpreted as the collapsed portions of what was once a much longer lava tube. Buried lava tubes are expected to protect human explorers as well as instruments from radiation storms as well as extreme variations in temperatures on the Moon's surface. While the day and night temperatures on the moon swing from +120°C to -180°C, and permanently shadowed polar environments are permanently colder than this range, temperatures inside the lava tube are expected to be at a near-constant -20°C near the equator (less towards the poles), which is relatively benign.

Figure 2.5. The Moon and a 1.7-km-long cave in Oceanus Procellarum. 3D images from Chandrayaan-1's Terrain Mapping Camera. A hollow lava tube with a cavernous mouth—about 120 meters high and 360 meters wide—and a roof estimated to be 40 meters thick.
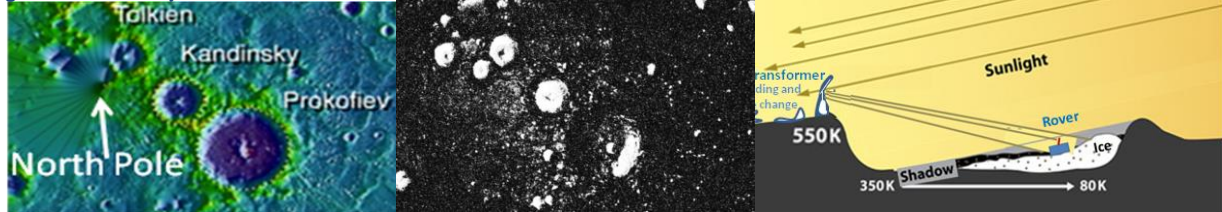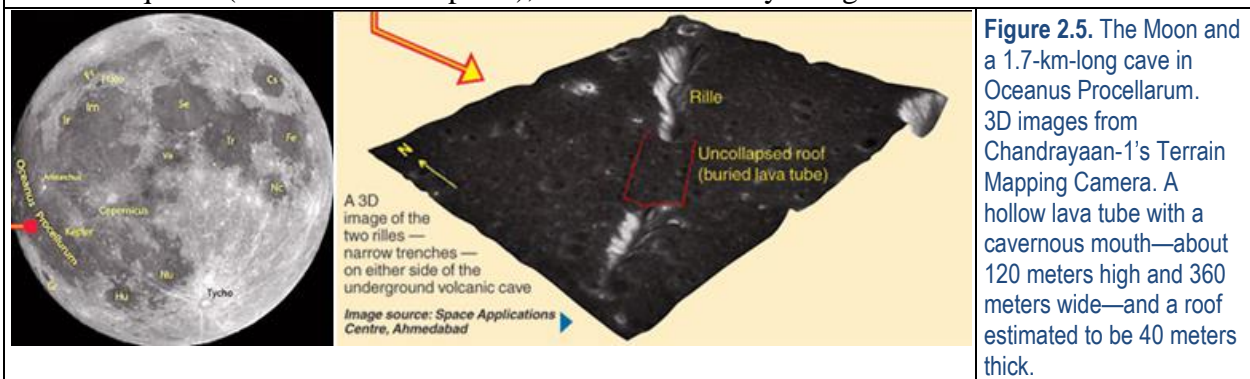
Science investigation Provide infrastructure to support multiple manned mission activities and precursor robotic reconnaissance.

Locale characteristics: Skylights and lower gravity imply larger-than-Earth tubes of order ~100 m typical diameter; negligible ambient lighting; likely rubble pile at access, but more smooth tube in interior; difficult (maybe vertical-drop) ~100 m depth access; long-wavelength (km-scale) sinuosity to tube; extensive dust; low-but-stable temperatures of ~-20°C.

Science and exploration targets; related questions: Primary goal is to provide a safe, stable environment for human activities. Secondary goals are scientific: (1) analysis of wall materials unmodified by space weathering; (2) dynamical and geochemical study of lava tube within flood basalts; (3) analysis of any volatiles trapped in the permanently shadowed cave environment; and (4) seismic studies for improved crustal structure.

Candidate known methods for evaluating scientific/resource questions: Seismometer—interior structure; stereo camera/flash—geology; spectrometer (UV/VNIR)—ice/mineral detection; UV fluorescence GPR—cave stability; mass spectrometer—carbon detection.

Environmental requirements that TF will have to account for: *Sunlight availability*: none inside cave, potential 1366 W/m^2 at surface daytime; *temperature conditions*: stable temperature of -20°C within cave near equator, more extreme variations at access point.

Requirements resulting from the science/exploration scenario goals: For manned mission, quite massive energy requirements, very sensitive to base design. For robotic precursor, ~100–200 W for mobility instrumentation, drilling, thermal, lighting; mobility solution at low TRL.

Typical rover design capabilities for similar environments and scenarios	Thermal environment for electronics and instruments. Mil-grade electronics would survive ok. Power/energy usage of rover/instruments, use of RTG.
"Gap" analysis	TF would provide a solution without RTGs.

2.4.4 Cave on Mars

Scenario: ER+TF are deployed near the entrance of a cave on Mars, to facilitate low mass robotic exploration of the cave. As caves provide unique environmental and ecosystem niches, these may be the best astrobiological targets on Mars. If there is net volatile deposition, they may also provide a unique insight into the martian climate record since formation.
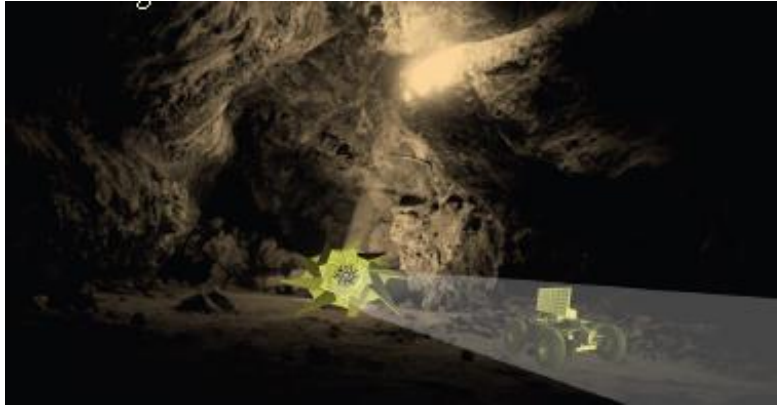
Figure 2.6. Cave on Mars with rover power by a sequence of TFs. Artist view.

Science investigation: Study of caves on Mars as an environmental and possible ecosystem niche, as well as a preservator of Mars' environmental and geological record since formation. Such an analysis could also be a precursor to a manned mission, as caves are relatively benign environments.

Locale characteristics: Skylights and lower gravity imply larger-than-Earth tubes of 10s of m typical diameter; negligible ambient lighting; likely rubble pile at access, but more smooth tube in interior; difficult vertical-drop (~100 m) access; long-wavelength (km-scale) sinuosity to tube; extensive dust; low-but-stable temperatures; high potential for ice deposits.

Scientific and exploration targets; related questions: Organics and life detection potential; good mineralogical and geological exploration; ice/mineral sampling and analysis; improved crustal structure via seismics; dynamical and geochemical study of lava tube formation.

Candidate known methods for evaluating scientific/resource questions (e.g., possible instruments): Seismometer—interior structure; 3D camera/flash—geology; spectrometer (UV/VNIR)—ice/mineral detection; sampling arm with drill + mass spectrometer—carbon detection; microscopic imager—microgeology and microorganism detection.

Environmental requirements that TF will have to account for: *Sunlight availability*: none in cave, ~600 W/m^2 peak daytime at entrance. Possible wind and dust outside where TF is. *Temperature conditions:* Somewhat variable, due to thermal transport in atmosphere, but approximating mean ground temperature in region. ~-50ºC near equator. Possible micro-environment weather within caves, potentially more humid than surface; dusty environment, tough on mechanisms.

Requirements resulting from the science/exploration scenario goals: ~100–200 W for mobility, instrumentation, drilling, thermal, lighting; mobility solution at low TRL.

Current typical rover design capabilities for similar environments and scenarios: RTG

"Gap" analysis: TF would provide a sustainable presence without RTGs.

2.5   Summary Conclusions from the Preliminary Analyses

The winds on Mars may affect the stability of projection, although for short distances of ~100 m down in a cave, and may not be an important deterrent. Inside caves one may need other repeaters—TF to project beyond LOS, deployed together with the ER. These two factors of added complexity (importance of stability, need for multiples) made us assign a high risk to focusing the refined analysis on a martian cave.

The lunar caves are relatively benign environments in terms of temperature. At -20°C, rovers do not need much heating—military-grade components are designed to withstand -55°C. The case for the projection of a micro-environment is not as dramatic. Moreover, the presence of the Sun is not as reliable as it is at the South Pole. The case did not appear as the best choice for test-casing the TFs.

Mercury craters are the most contrasting case of temperatures—many times more solar radiation than on the Moon and Mars, and about equally cold inside as in lunar polar craters. The higher level of solar intensity makes the problem easier than for the Moon, which may mean only limited applicability. TF operation in the higher temperatures of Mercury may induce additional problems. Finally, for all practical purposes, a lunar mission would prove the concept sooner, and the same technology would work with minor modifications on Mercury, with much smaller surfaces of reflection.

The lunar craters at the South Pole appear ideal for further detail of a mission scenario—no atmosphere, no winds, low gravity, a sufficient level of solar radiation, and regions are almost always sunny and very cold inside. The decision was to focus on this case for a mission refinement.

3   Lunar South Pole Crater Mission Scenario Analysis

A mission-specific analysis sets the stage for a set of system trade analyses in which to determine the design parameters for the TF (e.g., unfolded area, packed volume, mass reflective properties, pointing and shape controllability needs) for four primary functions of the TF: providing power to the ER solar panels, providing energy to heat the ER, maintaining the temperature of sensitive components in the operating range, providing illumination for in situ exploration and science operations, as well as providing a telecommunication relay.[1] The results of the system trade studies elicit a set of clear system-level requirements for the TF.

The mission concept is a lunar polar volatile exploration concept, specifically located in the Shackleton crater at the Lunar South Pole. A map of the South Pole region is shown in **Figure 3.1** [De Rosa]. We first review the conditions at the South Pole, focusing on the topography and solar illumination. We explore optimal locations for placing TF that get maximal exposure to sunlight, while also being on the rim to reflect it into the crater. We perform calculations for the needed size of TF for providing sufficient power to a rover traversing a crater, for a variety of rover sizes, power levels, and distances from the TF. We perform a thermal analysis for the TF and rover, which may have to survive cold for 2–3 days without solar illumination on its panels. We take a preliminary look at pointing dynamics and control, referring also to prior work on optics of non-imaging systems for efficient design of the pointing dynamics and control of the solar collection/relay concentrator [Wellford], with the intent to track the Sun and the rover. Points in proximity of Shackleton crater (e.g., Leibniz Mountain) have a continuous view of Earth and passive RF relays have been proposed in the past for that location, such that a base at Shackleton crater would have continuous communication with Earth.
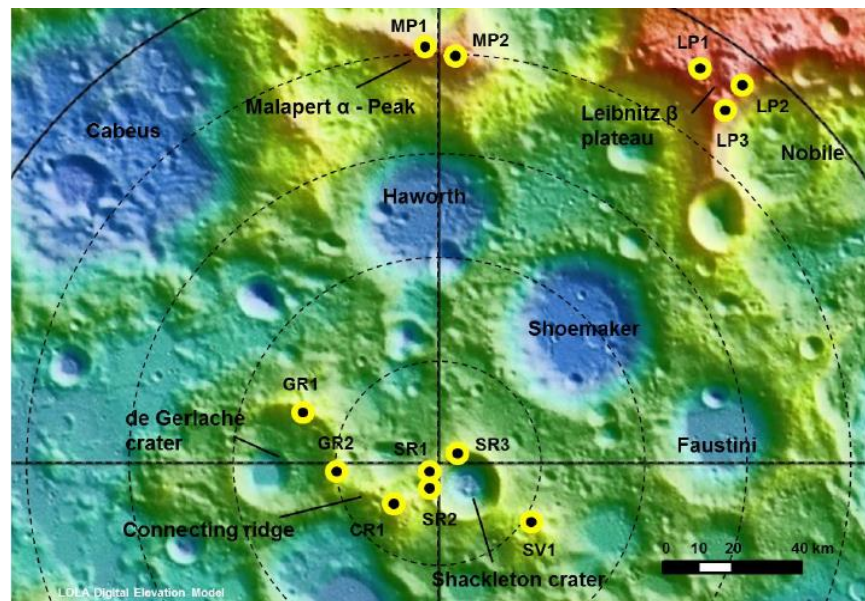
Figure 3.1. Map of the South Pole region based on a LOLA DEM. Isolines are every degree of latitude.

---

[1] The discussion uses material from [Shackleton], [Bryant], [Brandhorst] and [De Rosa]. The data used in these papers comes from the Goldstone Solar System Radar (GSSR) collected in 2006; and altimetry data from the Lunar Orbiter Laser Altimeter (LOLA aboard the SELENE spacecraft (Araki et al. 2009)). The tools used were at Astrium Space Transportation (Bremen), the John Hopkins Applied Physics Laboratory, and ESA. The results are consistent both with the Clementine earlier observations (1994) and with the Japanese Kaguya mission (2008).

The inclination of the Moon's rotation pole to the ecliptic plane is 1.54 deg. The Sun rises only a few degrees of elevation above the horizon and, in consequence, many crater floors are permanently shaded. However, taller peaks near the pole can see the Sun during the entire synodic month (29.5 Earth days, during which the Sun will appear on a full 360 trajectory).

As shown in **Table 1.1**, the intensity of solar energy falling on the lunar surface is about 1366 W/m^2, as on Earth and there is no atmosphere. Thus, there is no convection; conduction is limited due to the poor thermal conductivity of the regolith. Radiation is the only practical method of heat transfer.

3.1   The Environment at the Shackleton Crater

Shackleton crater (**Figure 3.2**) is located at center coordinates of 89.54°S latitude and 0.0°E longitude—the rotational axis on the Moon lies within the crater. The crater is approximately 20.7-km wide and 4.2-km deep. The slope towards the interior is about 30° downward towards the crater floor, 6.4 km diameter wide. The crater floor is never illuminated while the peak along the rim is illuminated by sunlight around 90% of the time. This makes the rim an ideal location for capturing/using the sunlight, in our cases, for the TF. Previous solutions were proposed for using solar panels that would convert light into electrical energy. Interestingly, the possibility of reflecting sunlight for illumination was also considered, without a detailed study. In plans that are now delayed for financial reasons, NASA has named the rim of Shackleton crater as a potential candidate for a permanent lunar base, to be continually manned by astronauts in not too distant future. A key reason for the choice is the water ice deposits, which can be used to produce oxygen, hydrogen fuel, and drinking water. **Figure 3.2** shows a topographic map of Shackleton crater and candidate base sites, points As and Bs [Bryant].
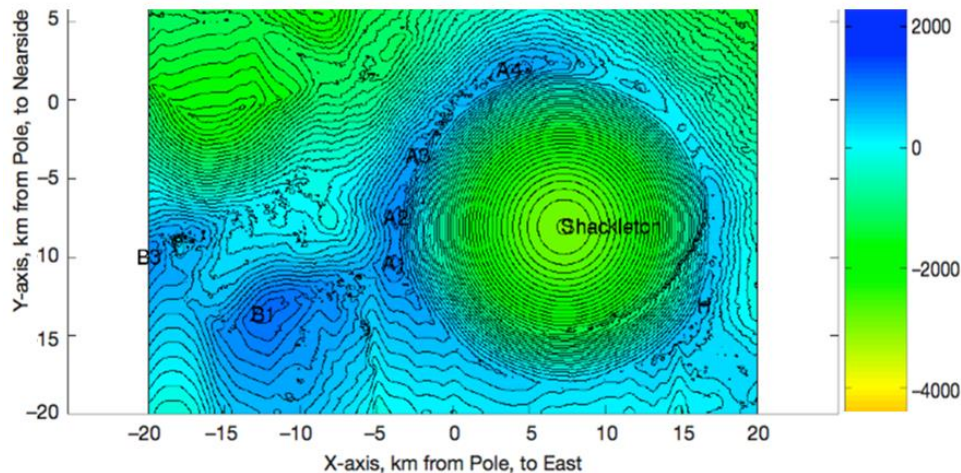
Figure 3.2. Shackleton crater topographic map, with base sites, taken from [Bryant]. The discussion will focus on points A1, A2, and B1.

Figure 3.3 shows the Shackleton crater map of yearly average illumination, showing almost permanent illumination on the rim. In this discussion, we will focus in particular on A1, A2, and B1, for which characteristics are shown in **Table 3-1** (from [Bryant]).
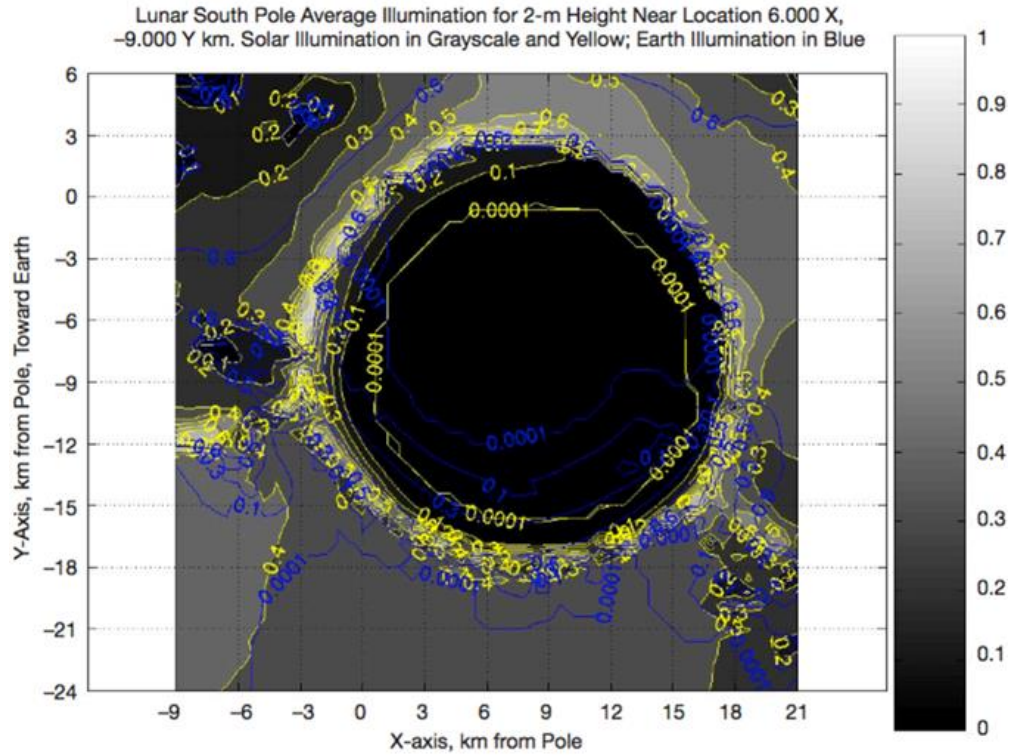
Figure 3.3. Shackelton crater yearly average illumination.

Table 3-1. Fine-resolution solar illumination statistics.

Site	X, km	Y, km	Multiyear Average Illumination (% of Sun Visible)			Months 100% Visible (% of Sun Visible)			Days Dark in Winter Month (% of Sun Visible)			Days Longest Continuous Darkness (% of Sun Visible)		
			(0)	(50)	(100)	(0)	(50)	(100)	(0)	(50)	(100)	(0)	(50)	(100)
A1	−3.720	−10.440	93.46	90.36	86.31	4.05	2.98	1.92	8.94	12.06	15.99	2.46	2.71	5.50
A2	−3.680	−7.520	92.98	89.47	84.83	4.46	3.40	2.34	10.58	13.70	18.29	2.63	2.79	3.04
A3	−2.200	−3.560	85.36	80.75	75.22	0.05	0.00	0.00	14.03	18.37	20.43	4.92	8.86	9.19
A4	3.720	1.910	87.83	83.66	78.51	0.00	0.00	0.00	13.21	17.06	19.85	6.23	7.63	9.92
B1	−12.400	−13.680	97.01	94.79	91.67	8.02	6.96	5.90	6.32	9.59	11.73	2.79	4.10	7.54

Multiyear illumination	0 % solar disk visible—the amount of time that any solar light is available; 50% solar disk visible—represents half-strength solar illumination; 100% solar disk visible represents the percentage of the multiyear interval with full solar power available.
Dark Days in Winter Months	Number of days during South Pole winter with less than specified % of solar disk visible. For 0% of solar disk visible, sum of days without any solar light.
Days Longest Darkness	Longest continuous period without solar power. For 0% of solar disk visible, this is the longest continuous period without any solar light. For 100%, this is the longest continuous period without full solar power.
Battery Storage Considerations	Worst case scenario: days dark in winter month associated with 100 pct of solar disk visible.

Thus, a summary of illumination, which varies with position around the rim of Shackleton crater is as follows (SR1 and SR2 are the notations in **Figure 3.1** from ESA mission paper, and correspond to literature points with literature name Site A.2 and A.1 [De Rosa].) The sites A.1, A.2, and B.1 (as designated in **Figure 3.1**) have the highest multiyear average solar illumination for the Lunar South Pole sites (Shackleton crater rim and west ridge).

- A1, the most lit area on the Shackleton rim, sees 100% of the solar disk 86.3% of the time. Longest period of continuous (total) darkness is 2.46 days; longest period of partial darkness (<100% solar illumination) is 5.5 days.
- A2, on the other hand has the shortest number of days without full Sun (3.04 days), with only slightly longer 2.63 vs. 2.46 days of total dark.
- B1 is a higher peak but with more days of total winter of darkness than A1 and A2.

Table 3-2. Illumination at SR1 (A.2) and SR2 (A.1).

ID	Region name	Longest illumination period [days]	Location (Lat/Lon [deg])	Literature name
Primary areas				
SR1	Shackleton Rim	274	(-89.7788, -153.4349)	Site A.2
SR2	Shackleton Rim	234	(-89.6871, -161.5651)	Site A.1

For the ridge connecting the Shackleton and de Garlache craters (Connecting Ridge, CR1), data from De Rosa plotted in **Figure 3.4** shows the path of the Sun above the local horizon. The area should be of similar appearance at A.2, with the Sun above the horizon almost all the time, and only obscured when a peak interferes its path.
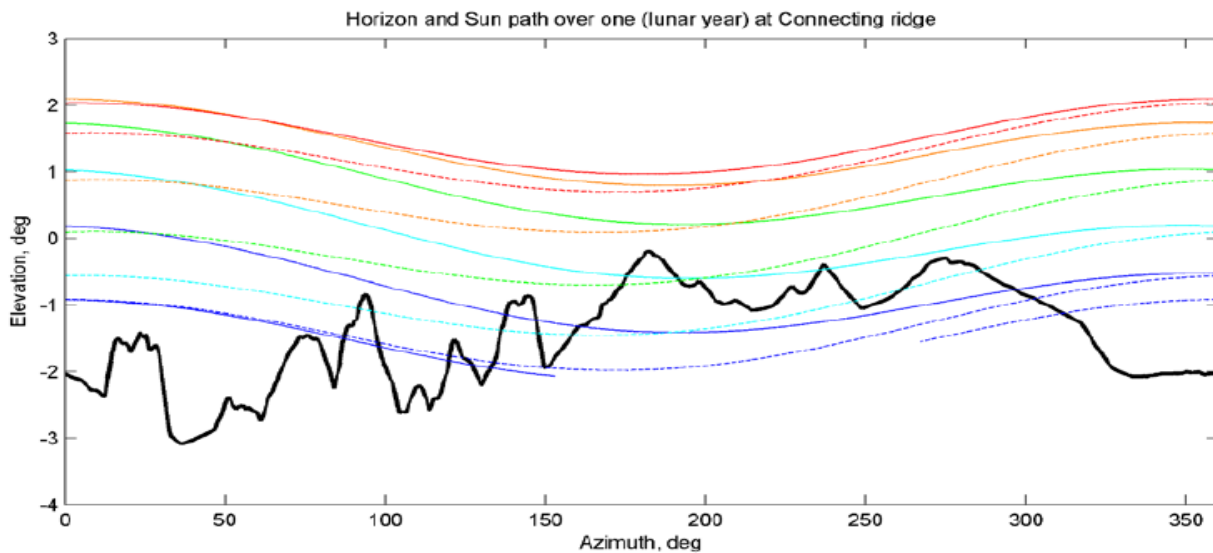
Figure 3.4. Local horizon (bold black line) and path of the Sun center over one year (color lines: red is summer, blue is winter), as seen from a location at Connecting Ridge (**Fig. 3.1**) around -89.5° latitude and 222° longitude close to A2 and A1, which would have a similar degree of Sun visibility [De Rosa])

Solar illumination increases with increased height above the terrain. **Table 3.3** shows different illumination metrics at different heights, at B1[2] (-12.400 X km, -13.680 Y km, elevation 1261 m).

For this location, Bryant uses data up to a few kilometers in height to illustrate increased illumination with height to mitigate the days of darkness, if needed, by raising a high tower. We only use, however, small heights since these provide sufficient percentage for our mission scenario and the improvement compared to complexity is not justified in our case.

Table 3.3. Solar illumination metrics for site B1 tower heights (selection of a few values, from [Bryant])

Tower Height (m)	Solar Illumination Statistics, Assumed Uniform Distribution Multilayer Average Illumination			Distribution from 2009 to 2028 Multilayer Average Illumination		
	0%	50%	100%	0%	50%	100%
2.0	97.01	94.79	91.67	97.08	94.89	91.99
32	97.60	95.67	92.69	97.71	95.79	93.03
64	97.89	96.15	93.41	97.98	96.27	93.78

The Shackleton crater rim also has a favorable position for continuous communication with Earth. While the best visibility to some part of Earth is around 65% and the entire Earth is visible about 50% of the sideral month, Shackleton rim has direct LOS with the peaks of Malapert Alpha and Leibnitz Beta (about 120 km away, seen in **Figure 3.1** and characterized in **Table 3.4**), which have at all times, 100% visibility of the Earth and can ensure a relay for continuous communication coverage to Earth. These relays could possibly be optimized/specialized TF.

Table 3.4. Location and elevation of Malapert Alpha and Leibniz Beta, with excellent visibility from Earth

Feature	Pole	X, km	Y, km	Latitude	Longitude	Mountain Elevation, km
Malapert α	S	3.56	119.60	−86.037	1.705	4.207
Leibnitz β	S	101.32	123.04	−84.723	39.471	6.055

3.2   Mission Trades

Mission trades were explored for a number of potential implementations of the TF/rover architecture. This was done to determine, at high level, optimal scenarios (minimal risk and cost). This included conditions for a single lander or two landers, as follows. The minimum risk scenario is then analyzed in further detail and illustrated schematically in **Figures 3.6 and 3.7**.

---

[2] Various studies refer to either A1, A2, B1 or Connecting Ridge but these are in proximity and with very similar characteristics to each other compared to the rest of the Moon.
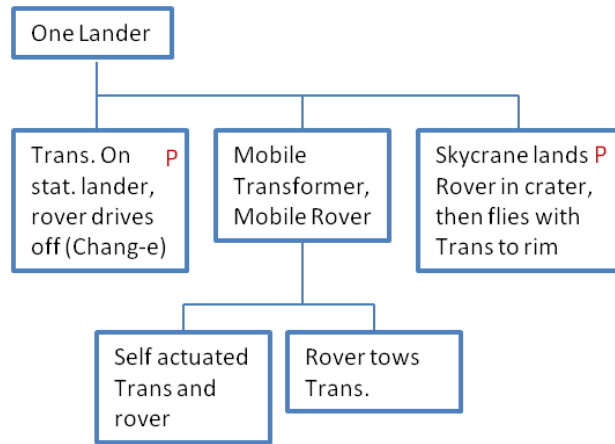
Figure 3.5. One lander mission trade P: requires precision landing.
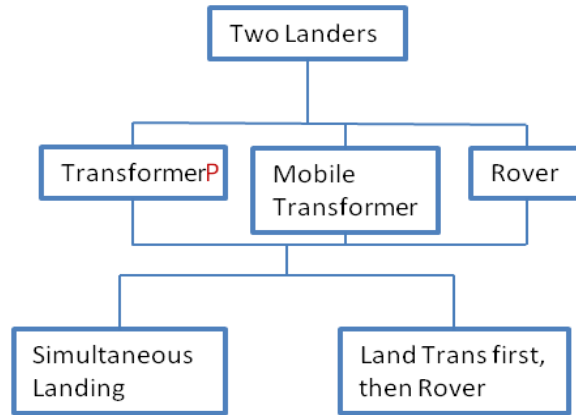
Figure 3.6. Two lander mission trade P: requires precision landing.

3.2.1 Single Landing

- Stationary lander/TF with mobile rover
  - Land on crater rim (precision required)
  - Rover must drive down into crater, maintaining view of TF
  - Probably least complicated and lowest cost
    - Biggest risk is visibility
- Mobile lander and rover
  - Land near crater rim
  - TF can drive (or be towed) to optimal position
  - Increased complication in flight system and operations
    - Significantly lowers risk, allows adjustment later in mission (if TF is self-motivated)
- Skycrane-type lander
  - Skycrane delivers rover to crater floor
  - Skycrane then flies up to crater rim and lands with TF (precision req.)
  - Increased complication in flight system and operations
    - Significantly lowers risk of getting rover down to crater floor

3.2.2 Dual Landers

Use of two independent landers can lower deployment risk

- Simultaneous landing of TF and rover
  - Can use either direct or low energy trajectory
  - Operations team must monitor two critical events near simultaneously
  - Rover would be on its own power until TF deploys and locks on
  - Staged landings use parking orbit at E-M L2 to delay second landing by ~1 month
  - Separate landings less taxing on ops team
  - Would allow transformer to land, deploy, and checkout before rover arrives
- Retains trade of precision landing of TF vs. mobility

The TransFormer crater mission design trade spaceshows the criteria used and the best option in each category (green) (**Table 3.5**). The overall best is boxed in red = lowest risk/cost.

Table 3.5. TransFormer crater mission design trade space.

# of Landings	One				Two			
Description	TF on stationary lander, rover drives off into crater	Lander delivers mobile TF and Rover	Skycrane delivers rover in crater, then flies TF to rim	Skycrane delivers TF to rim, then flies rover into crater	Mobile TF and mobile Rover		Stationary TF and mobile Rover	
Landing site	On crater rim	Near crater rim	Near and On crater rim	Near and on crater rim	Rover in crater, TF near rim		Rover in crater, TF on rim	
Precision	High precision	Low precision	High precision	High precision	Low precision		High precision	
Mobility (TF)	Static	Mobile	Static	Static	Mobile		Static	
Timing	Simultaneous	Simultaneous	Rover first, then TF	TF first, then rover	Simultaneous	TF first, then rover	Simultaneous	TF first, then rover
Trajectory	Direct or low-energy	Direct or low-energy	Direct or low-energy	Direct or low-energy	Direct or low-energy	Parking orbit at E-M L2 to delay second landing	Direct or low-energy	Parking orbit at E-M L2 to delay second landing
Operations	One critical event	One critical event	One critical event	One critical event	Two simultaneous critical events	Sequential critical events	Two simultaneous critical events	Sequential critical events
Risk	Med: Risk to mission if TF too far from rim; TF deployed, checked out before rover drives off; risk of rover driving down crater wall	Low-Med: TF positioned, deployed, checked out before rover drives off; risk of rover driving down crater wall	Med-High: Risk to mission if TF too far from rim; rover on its own power until TF is operational; lower risk of rover delivery into crater	Med-High: Risk to mission if TF too far from rim; rover on its own power until TF is operational; lower risk of rover delivery into crater	Med-High: Rover on its own power until TF is operational; lower risk of rover delivery into crater	Low: TF lands, deploys, checks out before rover arrival; lower risk of rover delivery into crater	High: Risk to mission if TF too far from rim; rover on its own power until TF is operational	Med: Risk to mission if TF too far from rim; TF deployed, checked out before rover drives off

3.3   Mission Scenario for Single Landing—Mobile TF and Rover

Figure 3.7 shows the elements of a mission scenario in which there is a mobile TF and a rover. A Sun-tracking heliostat redirects the light from the Sun into a projecting device (in a sort of periscope arrangement), which then redirects the light onto the rover. **Figure 3.9** depicts the scenario: the rover carries TF to the rim, TF deploys and illuminates rover panels, rover descends, TF continues to beam; folded TF after reaching the rim, starts unfolding, capturing solar energy, and reflecting into the rover.
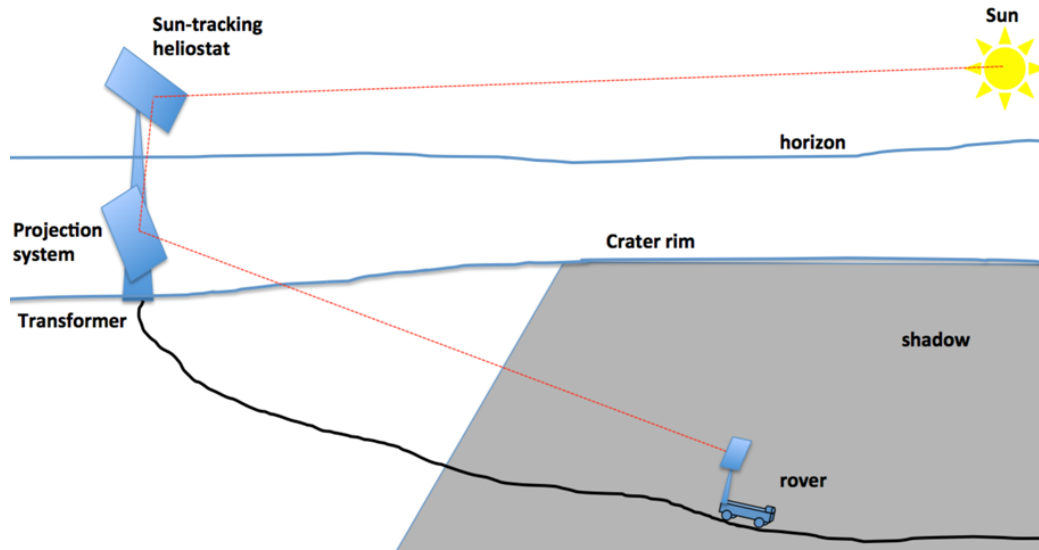
Figure 3.7. System model of TransFormer rover system on lunar pole crater.
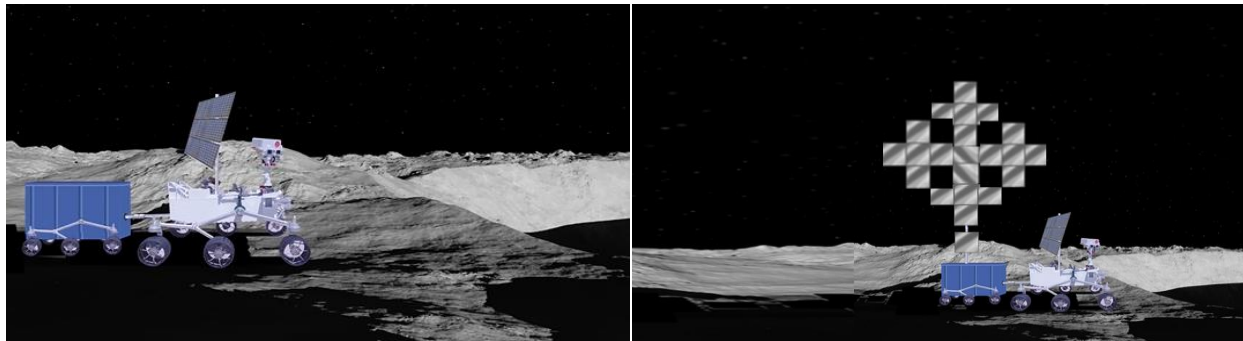
The rover makes its way out of the landing module, transporting a compactly folded TF, and approaches the rim.

The TF unfolds to reflect sunlight into the crater—it is placed at a location that provides line-of-sight coverage of the planned ER path, and, under its own actuation, adjusts its position/posture for improved stability, A crosslet origami unfolding is depicted.
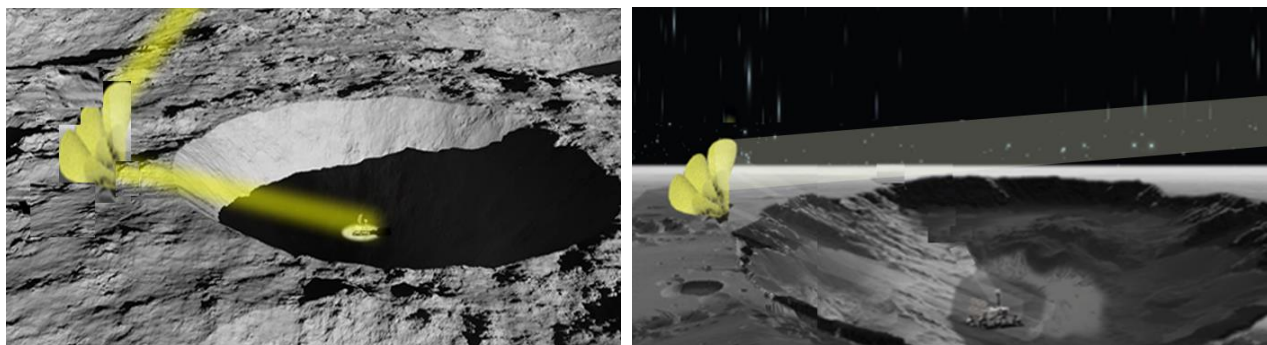
The ER starts its descent into the crater. The TF continuously tracks the ER, lighting its path with reflected sunlight. As the ER reaches areas with ambient temperatures below 100K, it is powered and warmed by the TF projected energy.

The TF continuously adapts its reflector shape, precisely tracking the moving ER, pointing the reflected energy onto its solar arrays, and controlling the beam as required for the ER to examine its surroundings and to take measurements.

Figure 3.8. Rover carries TF to the rim, TF deploys and illuminates rover panels, rover descends, TF continues to beam; folded TF after reaching the rim, starts unfolding, capturing solar energy, and reflecting into the rover.

3.4   Assumptions for Rover Characteristics

We consider three classes of rovers, within the range of parameters for electrical power needs, solar panel size, and radiative area indicated below. The values are rounded to define a class of vehicles, not to indicate the exact values in respective rovers, which are shown next to each other in **Figure 3.10:**

- MSL-class solar-powered rover (MSL): ~1000 kg, ~300 W power, ~4 m^2 of solar array area, ~10m^2 of radiative area on rover
- MER-class solar-powered rover (2004): ~200 kg, ~100 W power, ~1 m^2 of solar array area, ~3m^2 of radiative area on rover
- Sojourner-class solar-powered rover (1997): ~10 kg, ~25 W power, ~0.2 m^2 of solar array area, ~1 m^2 of radiative area on rover
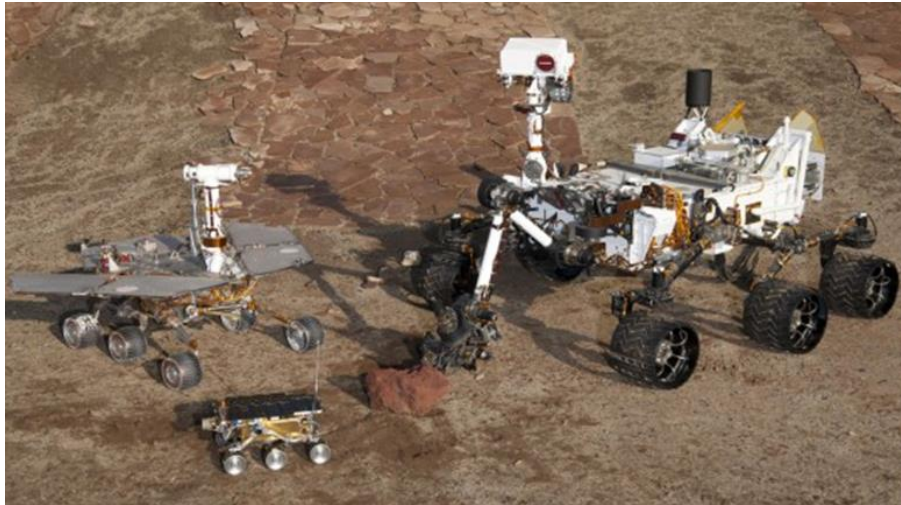
Figure 3.9. Three generations of NASA's Mars rovers in the JPL Mars yard.
Credit: NASA/JPJ-Caltech - Source: http://science.nasa.gov/media/medialibrary/2010/11/05/MSL-FEIS_Vol1.pdf.
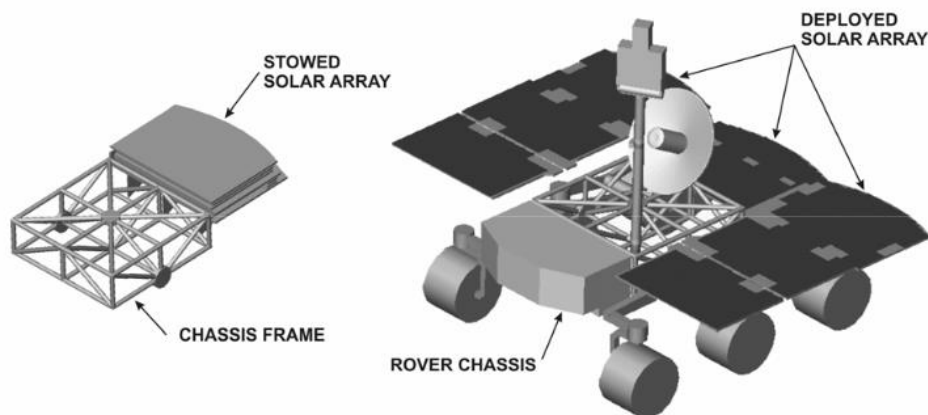
Figure 3.10. Illustration of a representative solar-powered Alternative 2 MSL rover.

The MSL rover for Alternative 2[3,4] would use a solar array as the source of electrical power for its engineering subsystems and science payload [JPL 2006]. The solar array would attach to the back section of the rover and would be folded for stowage inside the entry vehicle. The array would be deployed after the rover has landed on the surface of Mars. Representative stowed and deployed array configurations are illustrated in **Figure 3.16**. After landing, the solar array would be deployed into seven separate panels surrounding the rover on three sides and would be in a fixed position parallel with the upper surface of the rover chassis. The deployed array would have a surface area of approximately 6 square meters. The array would consist of the same type of multijunction solar cells as are used on the MER. At the atmospheric temperatures of the MER landing sites near the equator of Mars, this array would have a conversion efficiency of about 26%.

3.5   Optics Analysis

In this section, we summarize the optics analysis that was done as part of the JPL Team-A effort.

Illumination conditions for a rover with angular size (relative to mirror), less than that of the Sun (9.3 mrad). In this case, the rover only sees (illustrated with green beams) part of the Sun reflected, hence receives only a fraction of the incoming sunlight. (Likewise the Sun illuminates a considerable area around the ER.) This is shown in **Figure 3.12**.
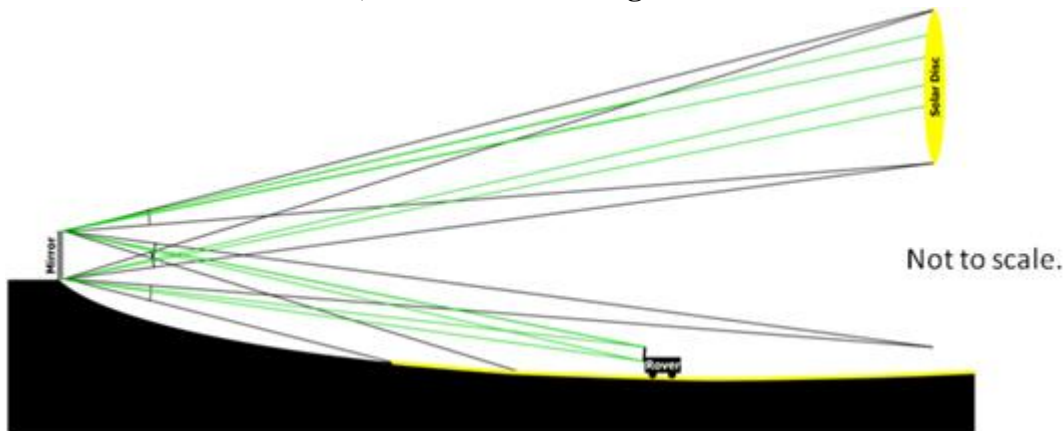
Figure 3.11. Ray tracing of the finite size of the solar disk onto the rover.

3.5.1   Desired Optical Requirements

1. The intensity of sunlight falling on the rover shall be the same as the solar flux at 1 AU (from this reference point one can determine proportionally smaller/larger values).
2. The maximum range to the rover shall be 10 km to reach the center of the Shackleton crater.

The solar intensity at some distance from the reflector depends on how much of the solar disk is seen in the reflector from a point at that distance.

3.5.2   Sun's Relative Intensity versus its Fractional Radius

The Sun's radius is 6.9598×10^8 m and the mean distance to the Earth's orbit is 1.496×10^{11} m, giving an angular diameter for the Sun of 9.3 milliradians (0.53 deg). The solar flux at 1 AU is

---

[3] JPL 2006. Jet Propulsion Laboratory. MSL Solar Feasibility Study. JPL D-33463, Pasadena, CA. March 20, 2006.
[4] Final Environmental Impact Statement for the Mars Science Laboratory Mission, Vol 1, NASA 2006.

1,353.3 W/m². The Sun's intensity (radiant emittance) is not constant across the disk of the Sun as seen from the Earth. This phenomena is known by astronomers as "limb darkening", and may be modeled by:

$$I(\theta) = I(0)[1 - u_2 - v_2 + u_2 \cos(\theta) + v_2 \cos^2(\theta)],$$

where:

$I(0)$ = radiant emittance at the center of the solar disk,

θ = angle between the normal at the Sun's surface and the line from the surface to the observer,

u_2 = 0.84 (best fit to data across all wavelengths), and

v_2 = -0.20 (best fit to data across all wavelengths).

The mean intensity is:

$$I(0)[1 - u_2/3 - v_2/2] = I(0) \times 0.82.$$

Figure 3.13 shows a plot of the Sun's relative intensity versus its fractional radius. Note that the intensity does not go to zero at the limb. The fraction of the solar radiant power is shown in **Figures 3.14** and **3.15**.
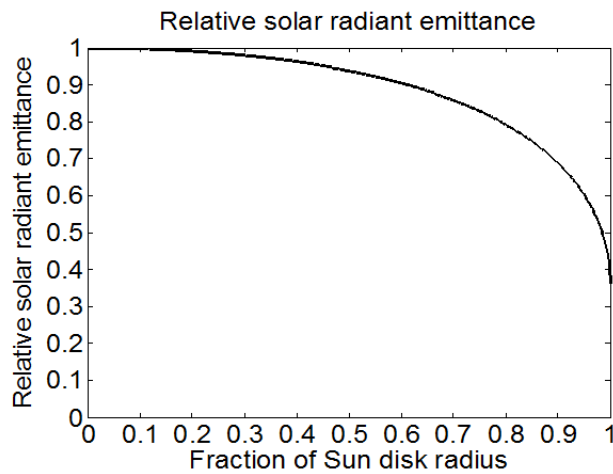
Figure 3.12. Relative solar radiant emittance.
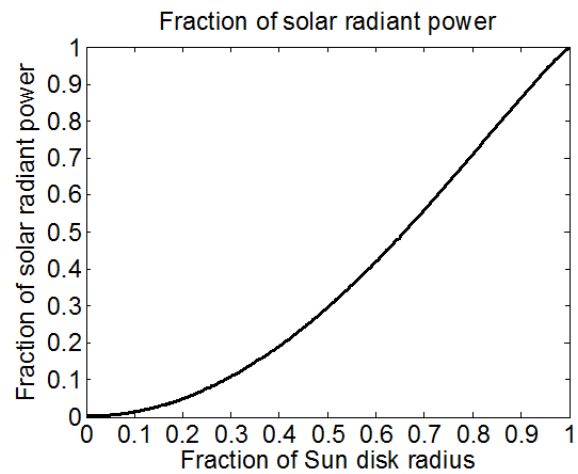
Figure 3.13. Fraction of solar radiant power.
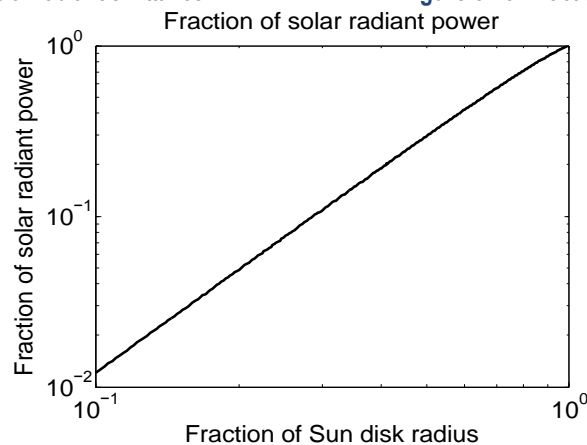
Figure 3.14. Fraction of solar radiant power.

If we observe the Sun through an aperture that is smaller than the Sun's apparent diameter, the relative solar radiant power is decreased, as shown in **Figures 3.13** and **3.14**.

The Moon's axis of rotation is inclined to the ecliptic plane by 1.54 degrees. Thus, from the point of view of a mirror near the South Pole of the Moon, the Sun would follow a circular path around the sky, no more than a few degrees above the lunar horizon.

3.5.3 Design 1: Two Flat Mirrors

The size of flat mirror needed to create 1353 W/m^2 at 10,000 m can be easily seen if we adopt the viewpoint of the rover. We wish to see the entire disk of the Sun through a circular aperture at a distance of 10,000 m. The diameter of this aperture is then 9.3 mr $\times$ 10,000 m or 93 m.

If we assume that the maximum reflection angle is 90 degrees (corresponding to an incidence angle of 45 degrees), then the mirror must be elliptical with dimensions of 132 m $\times$ 93 m.

Tracking the Sun through 360 degrees of longitude with an angle of incidence no greater than 45 degrees requires two mirrors. One possible arrangement is shown in **Figure 3.15**. While the Sun is in quadrant 1, light is reflected off mirror 1 to the rover; mirror 2 could also be used. For quadrant 2, the Sun is tracked by mirror 2, and the light is relayed by mirror 1 to the rover. For quadrant 3, sunlight goes from mirror 1 to mirror 2 to the rover. For quadrant 4, mirror 2 would be used, with mirror 1 as an alternate.
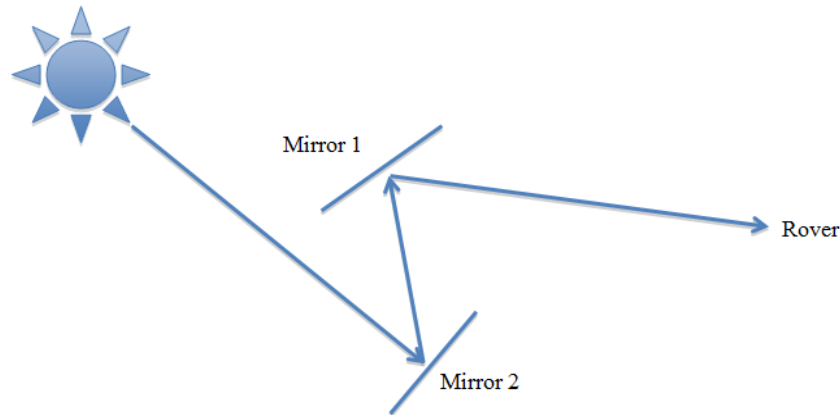
Figure 3.15. Tracking the Sun with two mirrors.

To derive the tolerance for the flatness of each mirror, regard each mirror as consisting of a large number of small, flat segments. The exact position of each segment or their number is unimportant; only the slope or tilt is significant. From the point of view of the rover, the portion of the Sun seen in any segment should not shift by more than a tenth of the solar angular diameter (i.e., 1 milliradian). This translates to a tolerance in the mirror segment tilt of 0.5 milliradian.

3.5.4 Design 2: A Curved Mirror and a Flat Mirror

By using a curved mirror, it is possible to concentrate the sunlight somewhat at a range of 10,000 meters. Again, this is best visualized from the point of view of the rover looking back at a curved mirror of many small segments. The tilt of each segment would be adjusted to view the center of the Sun's disk. The Sun's disk center has an intensity 1.22 times greater than the mean intensity across the entire disk. Thus, the mirror area can be reduced by 0.82 to give dimensions of 119 m $\times$ 84 m. The figure of the mirror would be approximately spherical with a 20,000-meter

radius of curvature. The angular range of motion would be ±45 degrees about a vertical axis and ±-12 degrees about a horizontal axis (to track the rover).

A second, flat mirror would be needed to track the Sun through half the lunar day (**Figure 3.16**). Its angular range of motion would be approximately ±-45 degrees about a vertical axis (to track the Sun through half a lunar day) and ±-0.8 degrees (to track the elevation of the Sun throughout the year). This flat mirror would be mounted higher than the curved mirror.
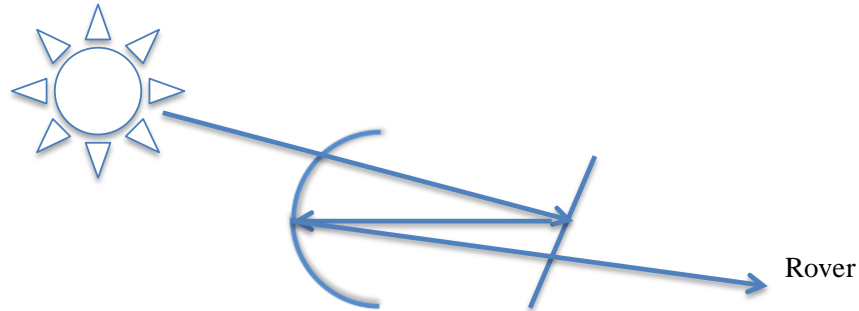
Figure 3.16. Overhead view of flat + curved mirror system for relaying sunlight to a rover.

The tolerances on each mirror will be the same as in the case of two flat mirrors.

3.5.5 Design 3: Two Curved Mirrors

The use of two curved mirrors (**Figure 3.17**) may allow for a better concentration of sunlight at the rover. To do a quick study of the possibilities, a simple, paraxial approximation, geometric ray-tracing analysis was done.

The best design found had these characteristics:

- Mirror 1: -1.01-m focal length (2.02 m radius of curvature) (yes, its convex), 1-m diameter (f# = 1);
- Mirror 2: 10-m focal length (20 m radius of curvature), 10-m diameter (f# = 1); spacing between mirrors = 9.0 m; and irradiance at 10,000 m = 18 W/m^2 over a 9.4-m-diameter area.
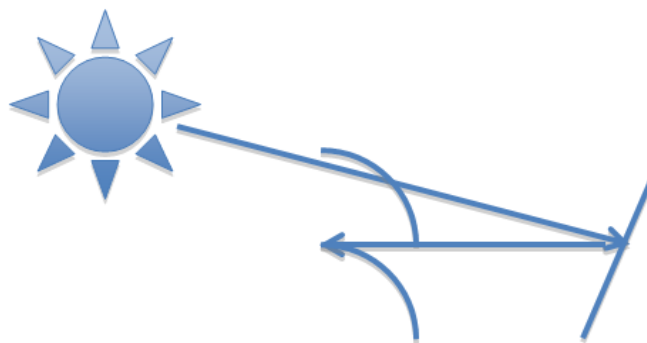
Figure 3.17. Overhead view of two curved mirror system for relaying sunlight to a rover.

These smaller mirrors could be stacked to form a periscope, thus simplifying the tracking of the Sun throughout the lunar day. The first mirror (on top) would rotate 360 degrees to track the Sun and reflect the light down a vertical axis to the second mirror. Mirror 2 would only need to pivot about two axes by a limited amount to track the rover. Due in part to the small f# of each

mirror, the tolerances would be quite stringent. To try and improve this situation, a design with two curved mirrors and one lens was investigated.

3.5.6   Design 4: Two Curved Mirrors with a Lens between Them

The best design from a simple, paraxial approximation analysis is:

- Mirror 1: 2.0-m focal length (4.0 m radius of curvature), 1-m-diameter (f# = 2);
- Lens: -0.109-m focal length, 0.12 m diameter;
- Mirror 2: 20-m focal length (40 m radius of curvature), 11.6-m-diameter (f# = 1.7)
- Spacing from mirror 1 to lens = 1.8 m;
- Spacing from lens to mirror 2 = 19.8 m; and
- Irradiance at 10,000 m = 13.3 W/m^2 over an 11-m-diameter area.

The tolerances in this design remain quite tight.

3.5.7   Discussion

The designs with multiple, powered optics did not produce a high enough irradiance at 10,000 m to justify their cost and complexity. The recommended approach would be to accept a lower irradiance than full Sun (perhaps 13 W/m^2) and use a flat mirror/curved mirror system with sizes 10 m × 14 m, stacked in a periscope-type arrangement. Due to the low tolerances, these mirrors could be constructed as a large number of flat segments made from a metallized plastic film mounted on a lightweight frame. **Figure 3.18** shows a plot of the solar irradiance vs. distance to mirror (left), and a plot of the solar irradiance vs diameter of mirror (right).

Reflecting the full irradiance of the Sun onto a rover at 10 km would require a very large mirror, on the order of 100-m diameter. This is because the Sun subtends an angle of 9.3 milliradians when viewed from the Moon, and the diameter required to cover this subtended angle (i.e., encompass the full disk of the Sun) when viewed from 10 km away is roughly 100 m (**Table 3.6**). Augmenting the system by appropriately curving the mirrors only buys us on the order of 10–20% benefit. So we would conclude from this that obtaining full solar irradiation will only work for Shackleton-sized craters if we leverage very large deployable or inflatable mirror concepts on the order of 100-m diameter, or if we can come up with a very low-power rover concept that can operate with roughly 100 times less power influx than we would expect in full Sun. The inflatable mirror option could be interesting in that it ties nicely to another ongoing NIAC project. Its main disadvantage comes from a lesser degree of controllability of smaller parts of its surface, which, in general, would be a desirable characteristic of a TF (also it may not be a good choice for a windy environment). Moreover, 1370 W/m^2 may neither be needed nor good for heating the terrain around the rover and sublimating the ice, but we will revisit this issue.

Figure 3.18, left, provides a plot of the solar irradiance vs. distance to mirror. If we consider a given efficiency of solar conversion on rover solar panels, and we multiply the area of the panels, we could obtain a similar number for the power generated by the solar panels. For simplicity, we use 16% efficiency and 6 m^2, their product being 1. Thus, the curves allow an easy reading—to obtain 300 W from rover solar panels, one needs a ~40-m diameter when at 10 km; at the same distance, one needs a bit more than 20 m diameter to obtain 100 W for a MER-class rover.
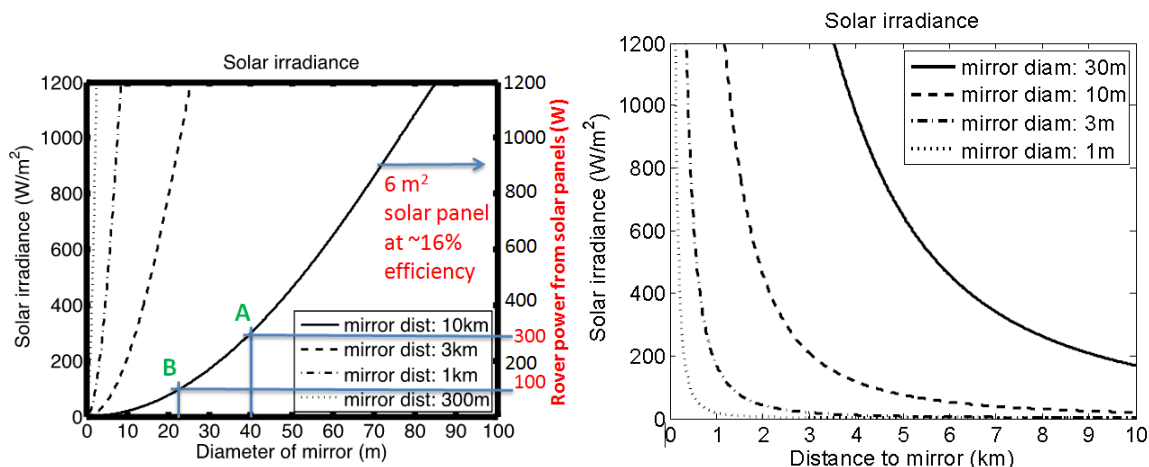
Figure 3.18. Solar irradiance vs. distance to mirror (left). Solar irradiance vs diameter of mirror (right).

Table 3.6. Lever of irradiation (W/m^2) at different distances, and for different mirror diameter.

Distance (km)	Mirror Diameter (m)				
	0.9	2.7	9.0	27.0	90.0
0.1	1300.505				
0.3	169.513	1300.505			
1.0	15.423	137.627	1300.505		
3.0	1.715	15.423	169.513	1300.505	
10.0	0.154	1.389	15.423	13.27	1300

3.5.8 Summary of Optical Study Findings

Key finding: The TF concept (as sized) will work for Shackleton-sized craters. Due to geometry of the problem, **powering an MSL-like rover at 10 km would require a reflector on the order of 40 m in diameter.** This assumes a conservative 16% efficiency in solar conversion (Mars Phoenix lander solar conversion efficiency was 26%), 6 m^2 solar array (increases in conversion efficiency will decrease solar array size); appropriately curved mirrors will buy additional ~10–20% benefit. Lower illumination level should be acceptable (e.g., MER) and can greatly reduce required TF size. Powering an MER-level rover would require a 25-m diameter. The calculated exact values are (at 10 km): 40-m diameter, TF would provide 286 W; 25 m diameter, TF would provide 113 W.

The TransFormer concept should be quite effective for cave exploration, where the rover is likely to be much closer to the TF, and thus a much smaller-diameter TF will reflect the full irradiance of the Sun. For reference, the following website has some relevant information about the physics of the problem: http://www.powerfromthesun.net/Book/chapter02/chapter02.html.

For even larger craters, an option to consider would be beaming concentrated power, possibly after an energy conversion, e.g. as laser, or microwave.

3.5.9 Use of Multiple Reflectors

A means of maintaining more constant illumination may involve using multiple mirrors to accommodate terrain. This may also change the area illuminated near the rover. As an example, assume two additional reflectors, A and B, where the distance from TF1 to TF2 is 5 km, and TF2 to TF3 is 50 m, and TF3 to the rover is 5 km (**Figure 3.20).** Assuming the size of the reflectors A and B is half the size of the TransFormer, the only losses come from reflectivity of the mirror

surface. Assuming a conservative 90% reflectivity, losses should be no more than 19% (81% transmitted).
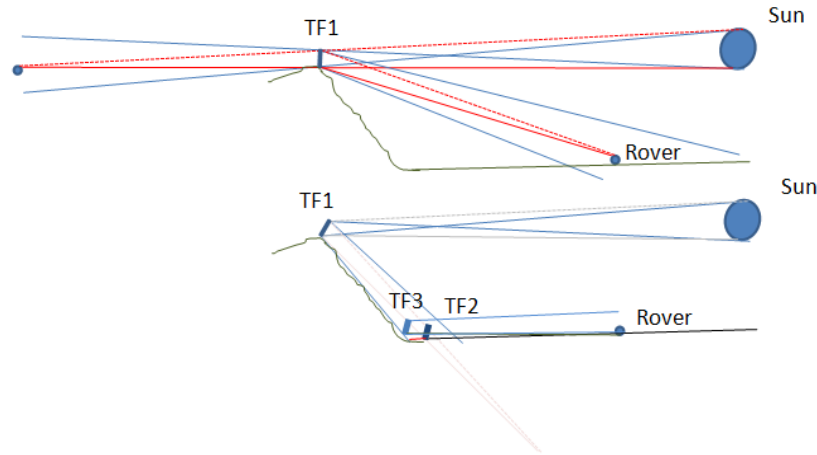
Figure 3.19. Direct and multireflector projection of sunlight to the rover. Note that the nearby area that receives the solar energy changes as well.

3.6   Rover Thermal Analysis and Findings

Next, we discuss the thermal analysis for the rover. Thermal analysis was performed for three sizes of rovers. **Figure 3.20** shows a snapshot of the tools used. Plots of worst-case temperatures of the rovers, the instrument payload, and the solar array, for both the case of the TF providing full solar irradiation, and the case where the TF is not providing any irradiation were determined. This clarified the temperature profiles with and without the irradiation from the TF, how long the rover could survive without the TF's irradiation, and conversely, how much heat would be required to keep the rover alive without the TF's irradiation (i.e., enable us to size the batteries needed for the rover). **Tables 3.7** and **3.8** summarize the findings.
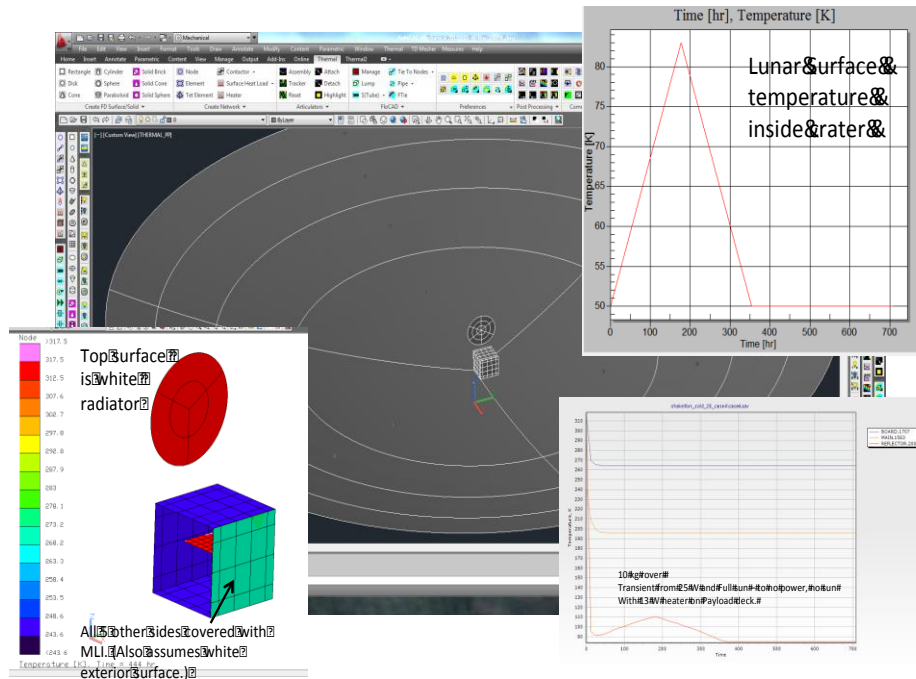
Figure 3.20. Thermal analysis at rover on bottom of crater.

The assumptions of the rover thermal analysis were: full Sun on solar panel and rover side, other five sides covered with MLI, and white exterior surface.

Table 3.7. Rover thermal characteristics and energy requirements.

Rover Mass	Thermal Power Req.	Energy Req.	Batt. Capacity (70% max DoD)	Approx. Battery Mass
10 kg	13 W	780 W-hr	1115 W-hr	11.2 kg (*unfeasible)
200 kg	30 W	1800 W-hr	2572 W-hr	25.7 kg
1000 kg	100 W	6000 W-hr	8751 W-hr	87.5 kg

- The conclusions of the thermal analyses are that rover thermal design is not an issue, provided:
  - There is an MLI blanket on the rover
  - Needed radiator area is minimized (a compact volume will lose less heat to space):
    - Qualify electronics to operate hot
    - Radiator efficiency will be reduced by lunar dust (anti-dust solutions are needed)
  - Use louvers to cover radiators to minimize heat leak during non-operation times
    - Reduces heater power needs
    - Extends time constant for cool down
  - Design mechanisms and structure for cold operations
    - Nighttime temperatures down around 70K
    - Drive and steering motors unheated
  - Warm-up heaters used on mechanisms prior to mobility operations in the morning
- Thermal control while illuminated should not be an issue using standard thermal control techniques (equivalent conditions to direct solar-illuminated rover)
- Assuming periods of total darkness up to 60 hours (2.5 days) battery capacity for survival heating would need to be as shown in **Table 3.7**
  - Note that battery mass unrealistic for 10-kg rover
  - Multiple transformers at different points on rim could greatly mitigate battery requirements

3.7 Comparison with Multi-Mission RTG (MMRTG) Power

Plutonium-238 in the form of plutonium dioxide has been powering MSL since August 2012.

Figure 3.21 shows the rover, with the MMRTG mounted on the back (right side of image), and MMRTG characteristics. **Table 3.8** shows a comparison of the TF with the MMRTG characteristics.

Power Level	Quantity (Beginning of Mission)
Thermal Power	1,975 W
Electrical Power Output	110 W
Physical Parameters	**Quantity**
MMRTG Mass	43.6 kg
Length/Diameter (fins)	66.8 cm/64.2 cm
Operating Life	At least 14 yrs

Figure 3.21. MSL MMRTG characteristics,
Source http://www.nasa.gov/sites/default/files/files/4_Mars_2020_MMRTG.pdf.

Table 3.8. Comparison of a TF solution with the MMRTG solution.

TF	MMRTG
Requires coordination of two independent autonomous systems	Allows single flight system (although communications satellite may be required)
Enables communication relay; could be continuous link	Requires relay satellite; intermittent link
Simplest variants require rover to descend crater wall	Allows landing directly in crater
Unlimited solar resource	Limited plutonium supply
Requires relatively complex operation and interactions: Sun and rover must be continuously tracked; rover must survive periodic outages in hibernation mode	Straightforward operation, tolerant of faults and communication outages
Provides area lighting, direct heating Rover power can be sized to need Can support large or smaller rover	Plenty of excess heat, but lighting requires electrical power. Provides ~110 W BOM (continuous). Must reject ~1900 W waste heat
Rover can be small / multiples Can be used for multiple missions	Mass ~**45 kg** per unit; implies large rover Costs ~**$45M** per MMRTG + $20M LA

3.8 Ice Sublimation Analysis

Vasavada et al. (1999) determined that it takes on the order of 15 min to heat a high thermal inertia surface from 100–170K by direct solar input (1362 Wm^2). In a different study, modeling by Andreas (2007) indicates that a 100-micron radius ice particle heated to 170K would only lose about 10% of its original mass in an hour. The floor of Shackleton crater is on the order of 40K and the solar input from the TF is on the order of 300 W/m^2. Thus, the time to heat ice particles would be longer, and so substantial sublimation of ice over a few hours time is not expected.

The following paragraphs provide more detail of the analysis in [Vasavada] and [Andreas]. **Figure 3.22** shows the ice sublimation rate as a function of temperature [Andreas]. The left axis gives the sublimation rate as a mass flux; its units are $\mu g\ cm^{-2}h^{-1}$. The right axis gives the sublimation rate as the number of molecules of water vapor leaving a square centimeter of the ice surface per hour at about 70K.
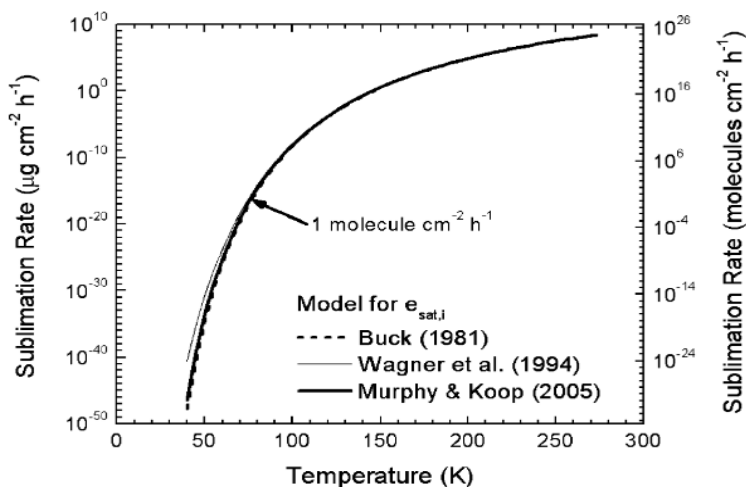
Figure 3.22. Ice sublimation rate vs. temperature

Source: http://www.nwra.com/resumes/andreas/publications/Icarus_Moon.pdf.

Ice deposits on the Moon might be "dirty"—for example, mixed with regolith dust, carbon dioxide, or some other contaminant (Nozette et al. 2001). Any such contaminants will lower the saturation vapor pressure of the ice and, consequently, slow its sublimation rate.

The fraction of initial mass (m0) remaining after time t when spherical samples of pure water ice with initial radii (r0) of 100 μm is shown in **Figure 3.23**. Initial calculations predict that a spherical lunar ice deposit of initial radius 1 μm would lose 10% of its initial mass in only 32 s if it were heated to 170K. A 100-μm-radius deposit, however, would require about an hour to lose 10% of its mass by sublimation if it were heated to 170K. Larger samples suffer even smaller rates of fractional mass loss.
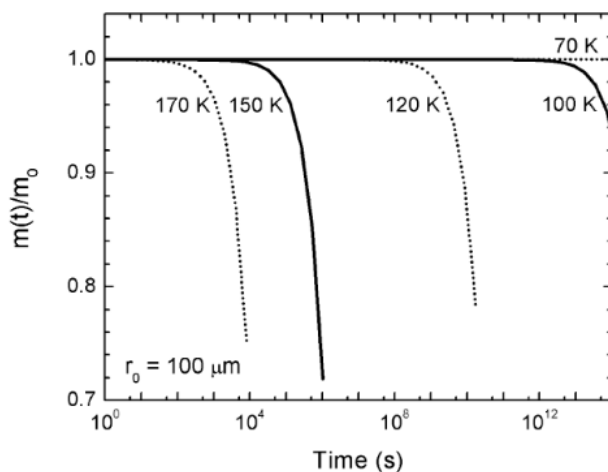
Figure 3.23. Mass of ice as function of time.

This summary evaluation (there is not enough information available for a good understanding of the nature of the regolith-ice mixture in the craters) indicates that the level of solar illumination taken in consideration by the TF (a reduction of about 25 times compared to direct solar exposure) would not have a significant impact if the projection lasts a few hours. However, the effects of long-term exposure are unclear and still of concern. This leaves two alternatives.

The first alternative is that the rover operates at the edge of the ice deposits, with potential illumination of an ice region controlled to a few hours, after which the rover returns to the safe, illuminated area. This is safe in two ways: the rover can benefit from the continuous power including when it goes over ice, and the projection is short enough not to induce sublimation.

The second alternative is to seek alternatives for more controlled projection and means to avoid projection on areas with ice. Both these alternatives require further study.

3.9   Thermal Analysis of the TF

Landis [Landis] described a technique for delivering photovoltaic power to a lunar base; it notes that the solar array on the moon will operate at higher temperature than arrays in near-Earth space. This is because the solar array operating temperature is determined by an energy balance equation, where the incident energy minus the energy converted into useful power is radiated thermally according to the fourth-power of temperature as specified by the Stefan-Bolzmann radiation law. The lunar soil is quite a good thermal insulator, and thus the solar array will be able to radiate to space only from one side. The operating temperature on the Moon can thus be estimated from operating temperatures in high orbit by assuming that the solid angle available for radiation is cut in two. The maximum operating temperature on the Moon will be increased by about 19%. Since typical operating temperatures for geosynchronous orbit arrays are approximately -305K, this yields a maximum operating temperature of 363K (decreasing slightly if the cell efficiency increases). This is very close to the temperatures reached by the

lunar surface at local noon. Average daytime power will be somewhat lower. These numbers are roughly consistent with those measured by instrument packages left on the Moon during Apollo. The large areas required for the solar array make it unlikely that cooling techniques will be usable. Since solar cell performance decreases with increasing temperature, a consideration in the selection of the solar cell type is to select a solar cell material which is not highly sensitive to temperature. More work on the thermal analysis of the TF requires constructive details and is proposed for a Phase II study.

3.10 Pointing and Control Preliminary Analysis

3.10.1 Heliostat Breakdown of Tracking Errors

Heliostat tracking technology is well established.[5,6] The tracking errors also depend on the Sun's position and rover position, and heliostat control is not a show-stopper.

Figure 3.24 shows the principle of heliostat Sun tracking to direct power to the rover. In this figure, it is shown that errors in the rover trajectory (errors in X and Y) as well as errors in tracking the Sun over the local horizon, combine to create the errors in control of the heliostat. Typical sources of errors, and their approximate magnitudes, in heliostat control design are, at least, for terrestrial applications. The numbers are indicative from a terrestrial application; the calculations for Shackleton crater will be done in the Phase II study:

- Pedestal tilt ~0.5 deg ; Non-orth. between az/el axes ~0.01 deg
- Mirror canting errors ~0.01 deg; Encoder resolution ~0.01 deg
- Azimuth and elevation bias errors ~0.25 deg; Errors in surface-relative location ~0.5 deg
- Gravity loading ~0.1 deg

$$2a = -d(t) + \operatorname{atan}\frac{Y(t)}{X(t)}$$
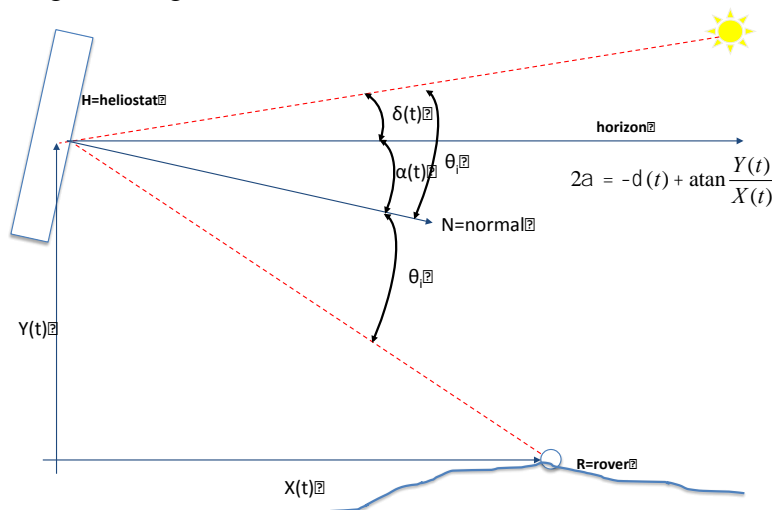
Figure 3.24. Heliostat tracking error principle.

3.10.2 Approach for Sensing at TF and Rover

From a sensing and control perspective, we expect that the following measurements need to be taken at the TransFormer:

---

[5] Baheti, Scott: Design of self-calibrating controllers for heliostats in a solar power plant, IEEE Trans. Aut. Cont., vol AC-25, no 6, Dec. 1980.

[6] Andraka et al: SANDIA capabilities for the measurement, characterization, and analysis of heliostat for CSP, SANDIA Report SAND2013-5492.

- Pose and location of TF with respect to surface frame (IMU, ephemeris with orbiter)
- Pose and location of each panel with respect to TF frame (laser metrology, encoders)
- Multiple-axis gimbal encoders to track Sun and Earth
- Temperature of each panel (thermocouples)
- Power of incoming sunlight (photodetector)
- Radio link with rover
- Radar/infrared detector to map dark area being engaged by rover

The following measurements need to be taken at the rover:

- Pose and location of rover with respect to surface frame (IMU, odometry)
- Temperature and illumination of received light (photocell, thermocouples)
- Radio-link with TF

Also, for purposes of inertial positioning and to redirect the light, we need estimates of how shadow progresses at the bottom of the crater, we need to know the local topography with hazard map, and we need temperature distribution in cold areas.

3.11   Science Value for Analyzed TF Mission Concepts

Large Craters: Distance ~10 km

TF Diameter ~40 m, MSL-class rover (300 W)

Instrumentation and Science: Stereo camera—geological analysis, traverse; spectrometer—ice/mineral detection; sampling arm/drill; mass spectrometer—ice, chemical, carbon detection; XRD—mineralogy; GPR—subsurface structure

Expected Value: Full geological and mineralogical exploration; ice/mineral sampling and analysis; subsurface structure

Mid-Size Craters: Distance ~3 km

TF Diameter ~5 m, Sojourner-class rover (15 W)

Instrumentation and Science: Stereo camera—geology; spectrometer (VNIR)—ice, mineral detection

Expected Value: First geological exploration of permanently shadowed craters; first-order mineral/ice detection

Deep Caves: Distance ~1 km

TF Diameter ~3 m, MER-class rover (100 W)

Instrumentation and science; seismometer—interior structure; stereo camera/flash—geology; spectrometer (UV/VNIR) —ice/mineral detection; UV fluorescence; GPR—cave stability; sampling arm; mass spectrometer—carbon detection

Expected Value: Good mineralogical and geological exploration; ice/mineral sampling and analysis; organics detection potential; improved crustal structure

Small Caves: Distance ~300 m

TF Diameter ~1 m, Sojourner-class rover (15 W)

Instrumentation and Science: Stereo camera/flash—geology; spectrometer (UV/VNIR)—ice/mineral detection; UV fluorescence

Expected Value: First cave exploration; ice/mineral detection

4 Feasibility Study of Transformers

4.1 Design and Operational Considerations for TF

The scenarios addressed in this study focused on TFs that provide solar energy to rover solar panels, as well as heat, illuminate, and act as a communication relay. They need to pack in compact form to deploy to a large surface, have good reflectivity, survive in the Sun, and be able to provide pointing and, in general, shape control, to embed autonomy for its operations.

Some general considerations for TFs are:

- Should use solar energy to power its own operation
- Should use a cellular/modular structure with largely similar modules (except a few possible exceptions), maxing the fabrication cheaper and the design more robust (by redundancy)

The specific requirements driving the design of the TF for the selected set of mission scenarios:

1. Compact volume when packed: less than 1 m^3, less than 1 m in each of the 3 dimensions;
2. Large surface when deployed: to a 40-m diameter, which is $20^2 * 3.14$, i.e., approx. 1200 m^2 (this means almost 1 mm thin, however, technologies below 100 microns are explored for the surface, with possibly thicker structural elements)
3. Low mass: less than 100 kg
4. Highly reflective surface (95% or better, with ~1 mm/m maximum surface deviation, tolerance in the mirror segment tilt of 0.5 milliradian)

4.2 TFs as Space Robotic Systems

Two elements that need to be clarified for the TF are their construction and their operation.

(1) TF 'anatomy', evaluating the capability of building a TF 'body' that would embed a diversity of functional primitives (reflector elements, solar cells, antenna elements, actuation, computation and control circuits), in a light, thin, flexible, multifunctional layer, yet with fine actuation;

(2) TF 'physiology', i.e., the means to execute its functions of computing, control, and actuation for shape change, the tracking of the Sun and ER and the precise pointing of energy reflection.

We follow the dictum 'the function creates the organ' since the subsystems need to match specific needed functionality, TF functions are summarized n **Table 4.1**.

Table 4.1. TF functions and means of providing it.

	Function	How	Action	Result
TFin1	Settle on the ground	Stable footprint, possible anchor	Place/anchor	Stable placement
TFin2	Self-power and prepare sun reflector (SR)	Increase surface facing solar radiation to max size needed by SP	Unfold, Generate Power	Energizer
TFin3	Thermo stasis Maintain/regulate temperature	Louvers, modify inclination/flip small reflective surfaces	Heat/cool	Thermo-stat
TFout1	Power rover solar panel (SP)	Track Sun and rover, and shape changing to reflect Sun to SP	Track, locate rover (beacon?)	Rover Heliostat
TFout2	Illuminate for the rover to see	Track Sun & illumination target	Track, locate targets	Illuminator heliostat
TFout3	Relay communications	Track orbiter & rover, shape change and relay signals	Track rover also orbiter	Orbiter Heliostat

Notations - SP: Solar Panel, SR: Sun Reflector, SC: Shape Change, SL: Sun Location, SC: Shape Change, RL: Rover Location, OL: Orbiter Location

4.3   Considerations for TF Design

4.3.1   Rotational Heliostat

A continuously operating photovoltaic or reflector power system needs to ensure efficiency as the Sun 'rotates' around the horizon. A rotational system is described in [Bryant]. **Figure 4.1** shows the heliostat design with a photovoltaic array installed horizontal to the local terrain. A parabolic mirror is installed above the array, in an angled position. This mirror is suspended from the crossbar of a mast next to the array. The mast could also be the structure for the lunar communications antennas. The mirror is suspended from an axle that is oriented parallel to the lunar spin axis. This axle rotates once per synodic month to continually reflect solar radiation onto the array.
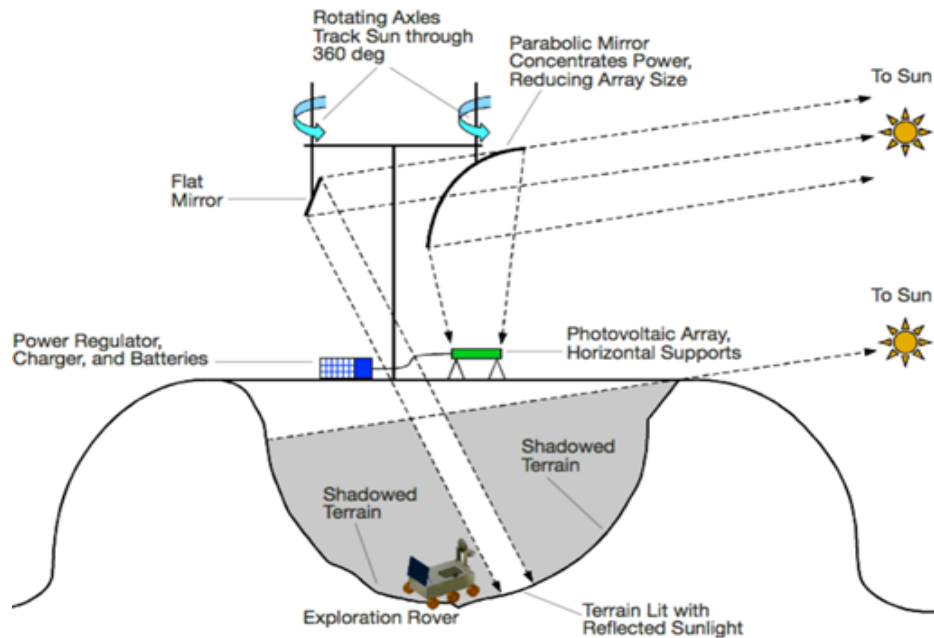
Figure 4.1. Perioscope mirror design [Bryant].

This heliostat "periscope" design provides continuous solar tracking. Shaping the mirror into a parabolic arc concentrates solar power for a small increase in mass. The trade-offs should consider the relative mass-per-unit area of the mirror and the photovoltaic panels, the reflectivity of the mirror material, and the relative masses of a rotating axle that supports the photovoltaic array versus supporting a mirror.

Bryant also described a TF-reflection functionality. Additional flat periscope mirrors mounted on the crossbar could be used to direct solar light to areas nearby. He considers this an efficient method of lighting work areas, which bypasses the inefficiencies of the photovoltaic system, battery storage, and electric lighting. If the photovoltaic power system is located on a crater rim (as in **Figure 4.1**), a flat periscope mirror could provide continuous lighting to exploration crews in the permanently shadowed areas within the crater. Sufficiently large heliostat mirrors could redirect enough sunlight to run photovoltaic arrays at remote locations. This would provide very efficient power transfer for operating within the permanently shaded areas. Transferring solar power with heliostat mirrors can also extend the mission operations time in the permanently shaded areas by removing the need to return to the base for recharging batteries.

4.3.2   A 3D Static Design of a Sun Collector

Bernardi and colleagues [Bernardi 2010, 2012] solve computationally and study experimentally the problem of collecting solar energy in three dimensions. They demonstrate that reflectors and absorbers can be combined in the absence of sun tracking to build three-dimensional photovoltaic (3D PV) structures that can generate measured energy densities (energy per base area, kWh/m^2) higher by a factor of 2–20 than stationary flat PV panels (no Sun tracking) for the considered structures, compared to an increase by a factor of 1.3–1.8 for a flat panel with dual-axis Sun tracking (see a design example in **Figure 4.2)**. The trade-off for increased energy density is the larger solar cell area per generated energy for 3D PV compared to flat panels (by a factor of 1.5–4 in their case).

This is an interesting avenue to explore for TF. Part of TF needs to obtain own solar energy and could use a static 3D design for it. Moreover, it may be possible that instead of optimizing collection of energy to optimize for directed reflection of energy. Some moving parts may still be needed since the rover position changes.

4.4   Foldable Structures

4.4.1   Stretched Lens Array (SLA)

A promising space solar array offering state of the art performance at low cost and ultra-light mass is the Stretched Lens Array (SLA) [Brandhorst]. The SLA uses a thin, flexible, linear

Figure 4.2. Prototype of a 3D PV. 3D mixed mirrors and solar cell structure optimize the conversion from a specific volume.

Fresnel lens optical concentrator to focus color-mixed sunlight onto multijunction solar cells (**Figure 4.3**). The lens is made by 3M using a high-speed, continuous, roll-to-roll process, from space-qualified silicone rubber material. For the SCARLET array and for the original SLA, the lens material was about 275 microns thick.
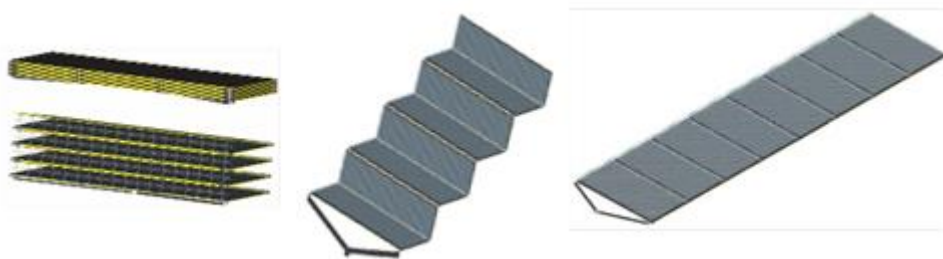
Figure 4.3. Stretched Lens Array.

4.4.2   ATK's UltraFlex

UltraFlex is an accordion-fanfold, flexible-blanket solar array comprising interconnected, triangular, ultra-lightweight substrates (gores). During deployment, the gores unfold and the array is tensioned to form a shallow, umbrella-shaped membrane structure.

UltraFlex is compatible with all solar-cell technologies, including the ultra-lightweight IMM cells anticipated to be ready for flight within the near future. The UltraFlex solar array is the state

of the art in terms of specific-power (W/kg) and stowed-power (W/m^3) density. What is also important is that it is customizable, and can be optimized for $/W, W/kg, etf. The UltraFlex wing stows to a much smaller volume and footprint on the spacecraft, and is inherently stiff and strong in its deployed configuration due to the efficiency of the tensioned blanket, supported by the backbone formed by the stowage panels. UltraFlex powered the successful Mars Phoenix Lander mission in 2008.
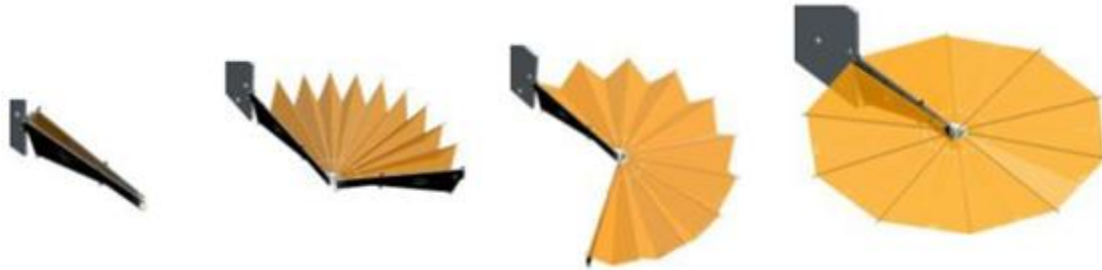
Figure 4.4. Accordion-fanfold deployment of UltraFlex.
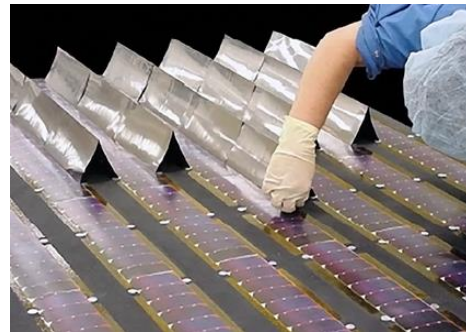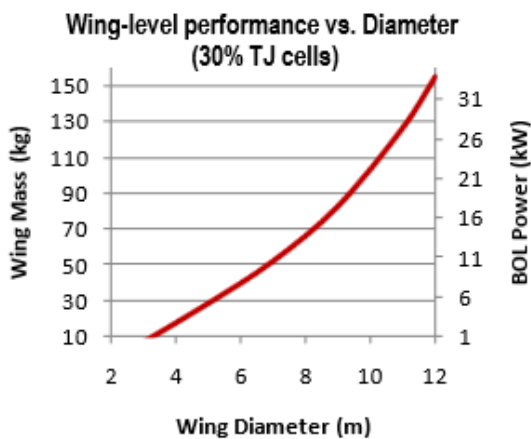
Figure 4.5. Scaling of UltraFlex performance and mass with diameter
Source: http://www.atk.com/products-services/ultraflex-solar-array-systems/.

Figure 4.6. CellSaver is an on-panel reflector that replaces every other row of cells.

ATK has demonstrated high performance photovoltaic concentrator technologies, including the successful demonstration of 7:1 refractive Fresnel concentrator technology on NASA's Deep Space 1. The CellSaver reflective concentrator functions at a 2:1 concentration for a direct replacement of 50 percent of standard PV cells, allowing a significant mass and cost reduction for virtually any solar array system. The 2× concentration is an ideal compromise to provide significant mass and cost benefits without incurring unique thermal management or array-pointing challenges (http://www.atk.com/wp-content/uploads/2012/09/CellSaver-2011b.pdf).

4.4.3   Origami Folding—Eyeglass Telescope

The Lawrence Livermore National Laboratory (LLNL) Eyeglass telescope used origami-folding for a large structure:
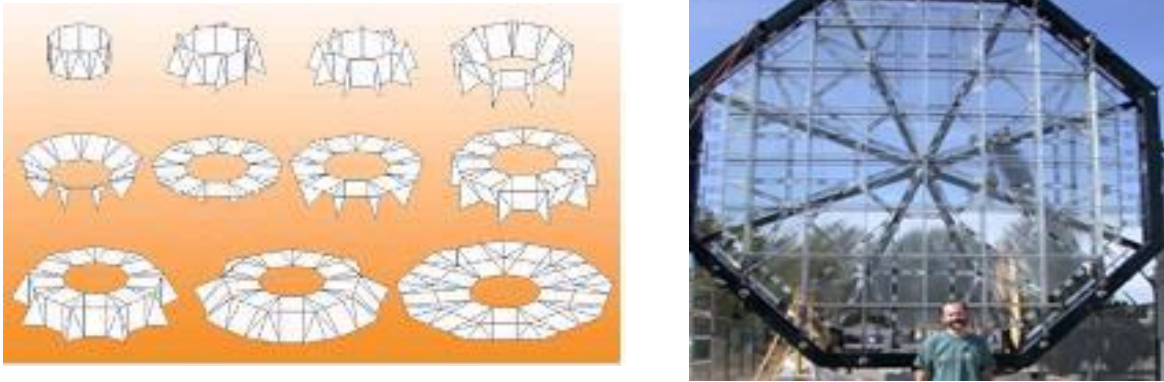
Figure 4.7. LLNL Eyeglass telescope.[7]

Helped by professional origami artist Robert Lang, scientists at LLNL designed a method for folding a space telescope so that it can be packed into a space shuttle and then easily deployed when in space. The foldable telescopic lens was called "Eyeglass".

In early 2002, a telescopic lens measuring over 3 meters in diameter was constructed. When folded origami style, it was 1.2 meters in diameter and shaped like a cylinder. By early 2004, a 5-meter prototype lens was constructed and shown to concentrate light as expected.

4.4.4   Miura Origami

Japanese scientists used origami concepts to pack and deploy a solar power array in the research vessel called Space Flight Unit (SFU) (1995). The solar array was folded into a compact parallelogram before launch; it was expanded into a solar sail once it reached space. The method of folding the solar panels is called "Miura-ori", in honor of inventor, Professor Koryo Miura, of Tokyo University (see **Figure 4.8)**.
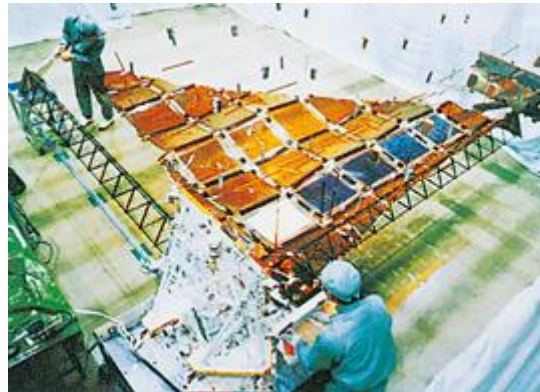
Figure 4.8. Miura-ori foldable solar panels at JAXA

Source http://www.isas.jaxa.jp/e/enterp/tech/st/07.shtml.

---

[7] http://www.langorigami.com/science/technology/eyeglass/eyeglass.php
Deployable Antenna http://www.faqs.org/patents/app/20120193498

The Miura-ori (translation = Miura-fold) allows a square piece of paper to be folded in such a way that it can be opened in one motion by pulling at two opposite corners; such a folded surface is less likely to tear at the crease junctions. Extensions of Miura-like folded surfaces are shown in **Figure 4.9.**
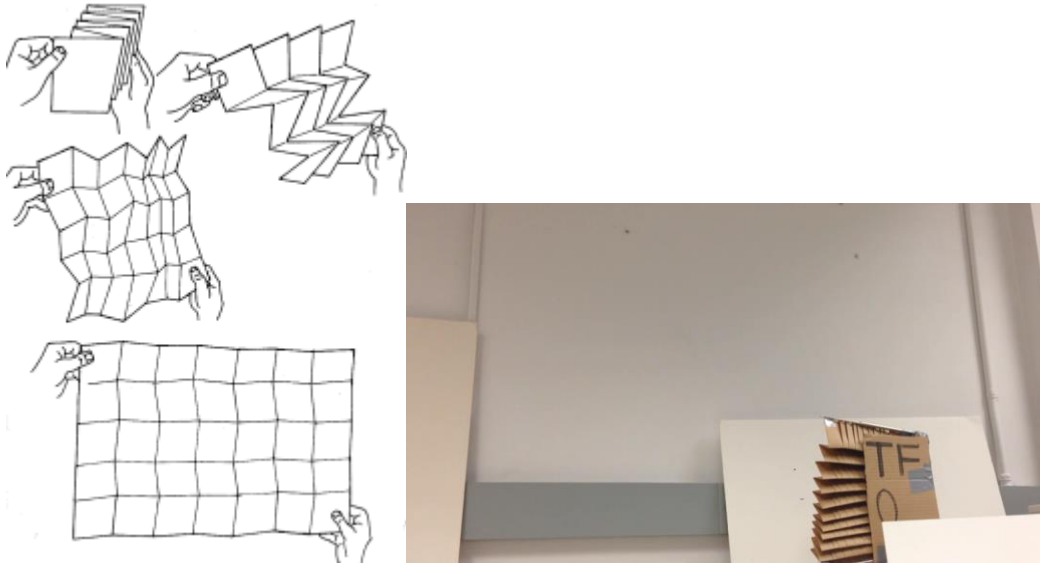
Figure 4.9. Telescopic expansion of a Miura-like folded surface.

Left diagram from http://www.origami-resource-center.com/origami-science.html). Experimental prototype at JPL on the right.

4.4.5   Programmable Matter—Origami Robots

Research funded by the DARPA Programmable Matter Program resulted in a variety of origami-robot prototypes, such as the one illustrated in **Figure 4.10.**
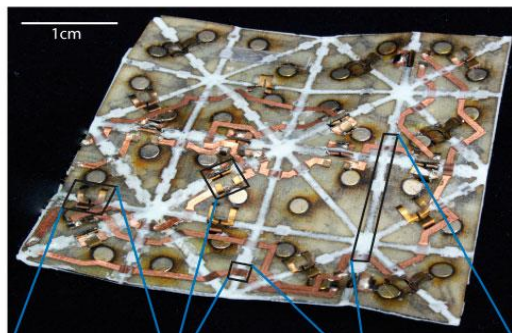
Figure 4.10. Origami style folding.
Credit: Programmable matter by folding, Hawkes, E. 2009.

4.4.6   The Crosslet Origami—A candidate Solution for TFs

We invented a novel origami folding TF in which we sought a configuration made of serially connected rigid bodies, with a repeating (fractal) pattern (a cross, as in **Figure 4.11**). This design would be repeated multiple times in order to obtain the desired size of the TransFormer. **Figure 4.12** shows the terminal unit, the 'bud' from which one opens the 'leaves', which will then perfectly fill the open spaces.
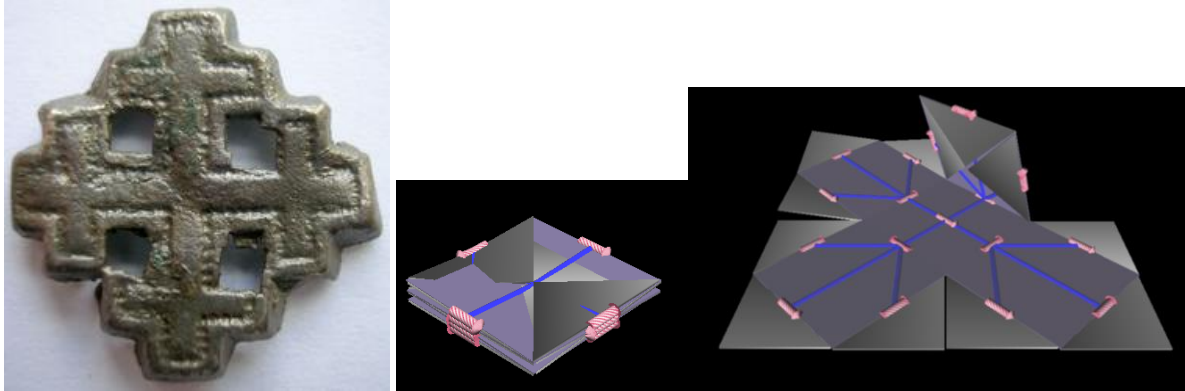
Figure 4.11. Copper-alloy mount of cross-crosslet shape of possible early 16th century date. Association with Order of the Knights of the Holy Sepulchre (left). The same fractal-like design (cross opening in smaller crosses, is used to unfold a large surface, as illustrated with 2 step unfolding on the right side).
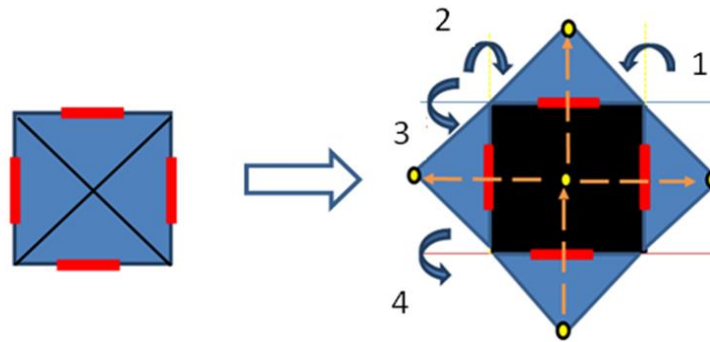
Figure 4.12. A terminal bud before and after opening the 'leaves'.

The design chosen uses a serial chain, a multibody system having interconnected rigid bodies. The rigid bodies, or links, are constrained by their connections to other links. The presence of closed chains is avoided for the purpose of reducing the complexity in the dynamic analysis of the model and thereby targeting more accurate and replicable results from the simulations. (In a closed chain the end effector or the last linkage is connected to its base by means of joint, which means that in order for the model to produce a valid solution, these linkages forming a closed chain must act together). The trade-off is that the closed chain system has additional rigidity for the same overall mass.

The design was modeled and a set of physical/dynamical simulations were performed. A feed forward control was implemented along with a Proportional Integral Derivative controller (PID) which calculates an "error" value as the difference between measured process variables and desired set points, and leads to minimal deviation during the deployment and shape changing of the TF. Simulations allow for a characterization of the behavior of the system based on the sequence of actuation of joints, allowing an observation of behavior under various speeds of operation.

The sequence of operation that governs the order in which the folds will occur is specified by implementing a Finite State Machine (FSM) in the simulation. The FMS allows the controls of the order of folding operation by scheduling the time after which the next operation needs to be executed. A Level-2TF consists of a 4-unit cell or level-one configuration TransFormers connected to each other orthogonally at one of the free corners. In total, a level two design consists of 4^2+1 rigid bodies and 4^2 pin joints.

The design has the capability of controlling each joint separately from all the joints present in the TransFormer. This will allow the TransFormer to carry out multiple functions simultaneously.

The approximately 1200 m^2 TF would be a level 5 topology (Fig. 4.13 right). This translates into the TransFormers consisting of 1,025 rigid bodies and 1,024 pin joints.
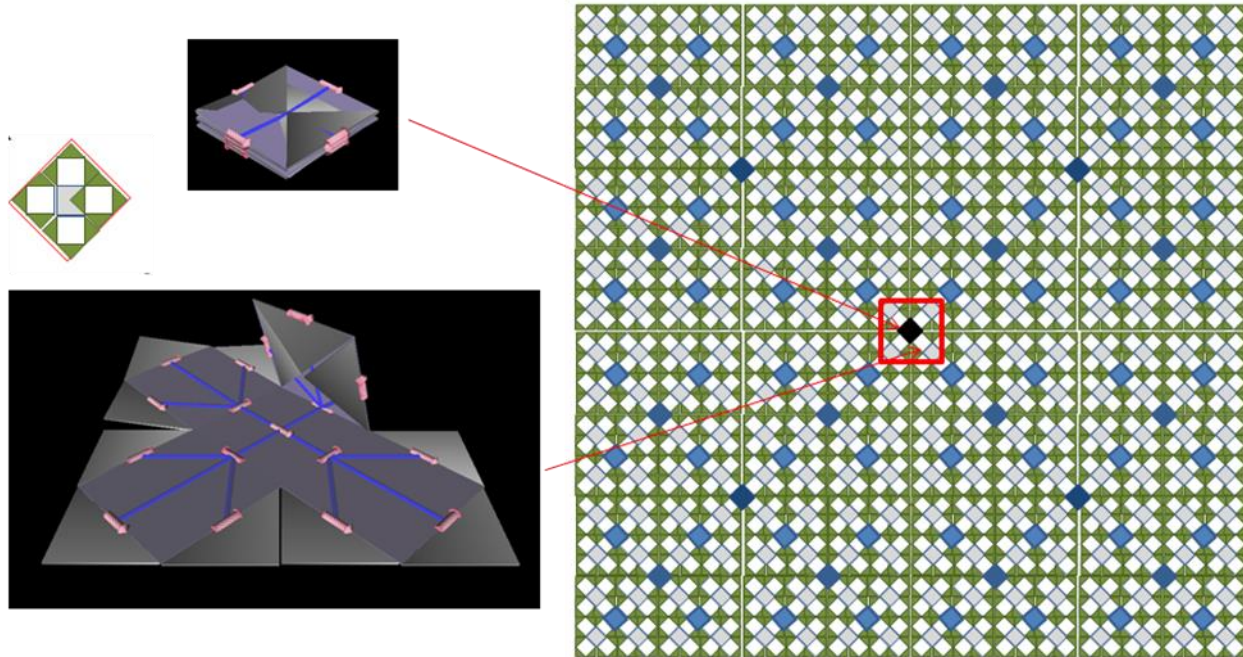
Figure 4.13. TransFormer Crosslet Origami topology Levels 1, 2 and 5.

4.5 Multifunctional Tiles

The following refers to aspects of <u>fabrication</u> of TF surfaces <u>on</u> a <u>thin</u> layer. To provide the desired suite of functionality, the TransFormer surface may need to be quite large, and yet, if thin, it could be packed into a small volume during flight. Assuming the mission allows for a 1-m^3 packed TransFormer, a surface of ~100 microns, can unfold to an area of 10,000 m^2, i.e., a 100 m × 100 m square. Made of a gossamer-thin, flexible, multilayer sheet, they may have one side covered with solar cells, and the other side with a highly reflective coating, while inner layers compute, self-actuates to change shape, store energy in batteries, and embed a spider-web antenna.

4.5.1 From E-Fabrics to TF-Fabric

A 40-m diameter TF allows for an effective surface of ~1200 m^2. Such a system, when stored in 100-μm thin packs, would only occupy a volume of 0.12 m^3 (40-m diameter – 20 m^2 radius 3.14*20*20 = 1200 m^2). Increasing this volume to 1.2 m^3 would achieve an unfolded TF diameter of over 60 m (or could allow for a 40-m diameter TF with a thickness of 1 mm). The large area of the TF fabric enables engineers to think differently about the ways in which computation are distributed over the large, multipurpose TF fabric that would normally be computed using traditional discrete components. The specific functions that the thin, flexible TF fabric is expected to perform includes:

- Energy collection
- Energy storage

- Energy redirection
- Unfolding and fine-grained actuation
- Sensing
- A level of computation and control
- Communication to the ER and an orbiting satellite

All of these subsystem functions have been individually demonstrated on thin flexible layers (<100 microns), of tens of microns: power from solar arrays [9, 10], avionics circuits [11], controls [12], sensing [13], shape-memory alloy actuation [14], communication circuits [15, 16], and antennas [17, 18].

The density of integration for thin, flexible layers is lower than those of rigid substrate. While this limits the applications for which these technologies can be applied for typical applications (e.g., consumer electronics), this is less of a concern for TFs, due to their large available surface areas exceeding 1200 m². The discussion is maintained for a flexible substrate for generality, although rigid square tiles, e.g., of $1m^2 \times 1m^2$, would be a feasible alternative.

4.5.2 *TransFormers Low-Grain Cellular Structure*

The TF fabric can be broken down into discrete functional regions responsible for different functions necessary for the operation of the TF. These functions, described briefly above, include actuation, energy manipulation, sensing, and communication.

Actuation

Actuation of the transformer is necessary for two of its distinct phases of operation. The first involves large, not so often movements related to unfolding from its packed shape to its fully unfolded shape. Initial unfolding is expected to follow an origami-type approach that enables the final structure to resemble a diversity of 3D structures. (Partial folding back may be needed in certain cases, e.g., on Mars if one wants to avoid the effects of a wind storm.) Work in these areas for specific subsystems has been done under *programmable matter* [21] and *origami robots* projects [22]. Subsequent unfolding and shape change second involves smaller actuations for Sun and rover tracking.

Potential implementations of actuators include electroactive polymers (EAP), shape-memory alloy (SMA) [14], and piezoelectric bimorphs (**Figure 4.14**). SMA actuators are particularly well suited to the task of unfolding the TF fabric due to their small size and large range of motion. The associated fatigue from repeated use of SMA is mitigated due to the one-time-use nature of SMA components for unfolding. EAP and piezoelectric bimorphs enable repeatable motion suitable for Sun and rover tracking.
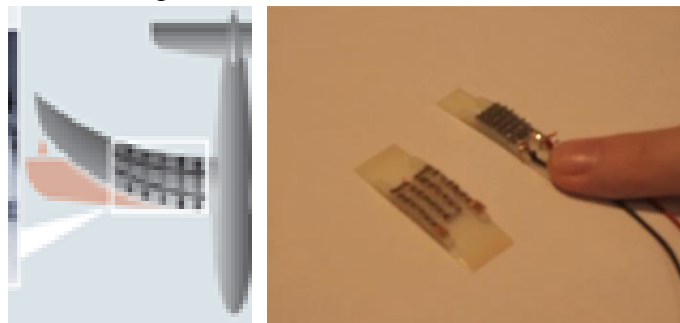

Figure 4.14. Shape-memory alloy actuation [14], piezo-electric materials under test at JPL.

4.5.2.1 Reflectors/Mirrors

The folded nature of a TF necessitates the use of individual components for its reflective surface. Origami folding of individual components to produce a large-scale unfolded structure was explored by LLNL for the Eyeglass telescope [23]. Additionally, the European Southern Observatory plans to build a 40-m European Extremely Large Telescope (E-ELT) telescope with a main mirror 39.3 meters in diameter. The main mirror is designed to be composed of about 1,000 individual, hexagonal modules, about 1.4 m wide and 5 cm thick. For a secondary, deformable mirror, the French company SAGEM has delivered a module—1.12 meters across and 2 mm thick—that is thin enough to nearly act like a flexible film. The reflective surface of the secondary mirror can be constantly altered by tiny amounts to correct for the blurring effects of the Earth's atmosphere resulting in significantly sharper images (**Figure 4.15**).

Figure 4.15. Thin-shell mirror made by SAGEM.

Sensing and Control, Computation for Pointing and Tracking

The TF fabric provides a novel method of large-scale distributed sensing and computation. Thin film technologies are able to produce sensors capable of measuring diverse information from the environment including temperature, force, light, and acceleration. The large area of TF fabric enables a large amount of data to be collected about the environment with capabilities for stereo disparity. However, processing becomes markedly different from traditional integrated circuit (IC) approaches characterized by high density, high frequency synchronous computation. Thin film Complementary Metal Oxide Semiconductors (CMOS) technology currently lacks density as demonstrated by ThinFilm's 20-bit memory cell. Nevertheless, the large area of the TF fabric compensates for some of the lack of density of the system. Additionally, the difficulty of synchronizing a 1200 m^2 TF fabric is irrelevant when exploring alternative neural network– and cellular-automata–based computing approaches. Here, computation is distributed across regular processing elements with local connectivity. Modern neural network-based approaches achieve high accuracy for potentially difficult problems related to ER tracking (object recognition [Hinton 2006]) and environment analysis (scene labeling [Farabet 2013]. Certain classes of these neural networks, once trained, operate in a strictly feed-forward manner. This type of processing is highly favorable for TF fabric, which naturally exhibits a feed-forward structure where data is moved from distributed sensors through increasingly complex levels of computation. **Figures 4.16 and 4.17** show computational circuits on thin flexible layers. The TF needs mechanisms to track the Sun, the rover, and the orbiter, and consider the actuation requirements to point to all these targets simultaneously during the course of one solar day.
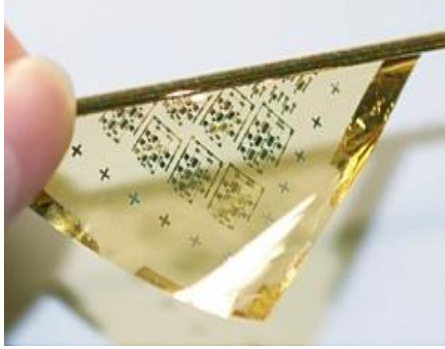
Figure 4.16. Analog and digital circuits on thin flexible layer.
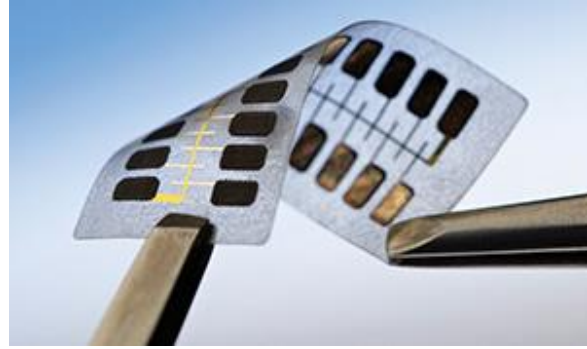
Figure 4.17. ThinFilm 20-bit memory cell.

Power

Power subsystems of the TF can be categorized into systems related to energy harvesting and energy storage. While thin film photovoltaics (TFPV) lag behind traditional, crystalline solar cells from an efficiency perspective (though not from a combined cost-energy perspective), certain emerging technologies are showing extreme promise with regards to efficiency. Perovskite PVs have recently achieved, in 2014, an efficiency of 17.9% [Ryu2014], up drastically from 3.8% five years prior. They are consequently rapidly climbing the National Renewable Energy Laboratory (NREL) efficiency charts, as shown in **Figure 4.18**, towards a maximum theoretical efficiency of 31% with higher efficiencies possible for multijunction devices. The simplified manufacturing techniques and costs required for these emerging PVs has the potential to enable high energy efficiency, reliability, and low cost for a large solar energy harvesting array incorporated into an unfolded TF.

In addition to energy harvesting, it is also necessary that a TF incorporates energy storage capabilities within its thin film fabric. Specifically, the introduction of capacitors and/or batteries into the TF fabric is critical for sustained operation of the TF in the absence of an RTG solution. Current research into thin, bendable batteries includes a variety of chemical substrates including traditional Li-ion batteries (LIB) [Koo 2012], LiS-based devices [LI 2012], and NiF_2-based devices [Yang 2014]. These systems can achieve comparable energy density to Li-ion batteries (~200 Wh/kg), but in a thin film package. Nevertheless, the actual energy storage of thin film batteries is limited by the available area that can be dedicated to a battery. For a traditional consumer application, a battery with an area of $1\,m^2$ would be exceedingly impractical. However, the large available area of the proposed TF fabric (i.e., $1200\,m^2$) enables thin film batteries to be manufactured and used in sufficient large areas to make them practical for powering the actuation, sensing, and communication systems of the TF. The $2.2\,Wh/m^2$ of [Koo 2012], when scaled up to $100\,m^2$ without layering, or approximately 10% of the available TF fabric, can achieve the comparable storage of a 1 kg traditional LIB. A flexible LIB and an NiF_2 based device are shown in **Figures 4.19** and **4.20**.

Figure 4.17. NREL chart of solar cell efficiencies.
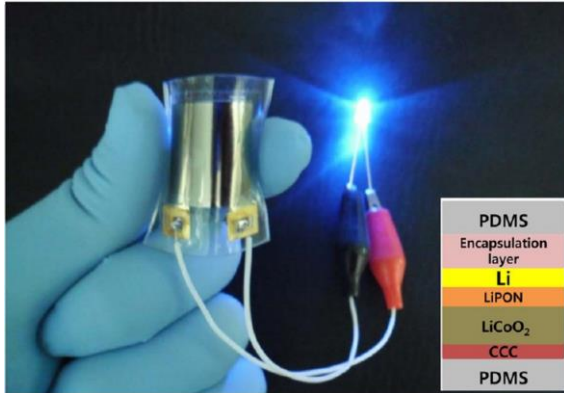
Figure 4.18. A flexible LIB capable of powering an LED [Koo2012].

Figure 4.19. A thin film battery using a NiF_2 process [Yang2014].

4.5.2.2 Communication

Communication strategies for the TF can be achieved through traditional RF antennas. Kingsley has demonstrated a MEMS antenna deposited on a flexible substrate that can be configured to operate on frequencies of 2.4–18 GHz [Kingsley 2007]. Additionally, Pulse Electronics has shown a translucent antenna less than 200 µm in thickness for consumer electronics applications. Such antennas, composed of transparent conducting oxides (TCO), are of high benefit for a TF system with multifunction stacking (as discussed in the next section). TCOs allow for light to be transmitted to lower layers while not sacrificing potential antenna area. Other papers for circuits are [15, 16], and for antennas [17, 18].
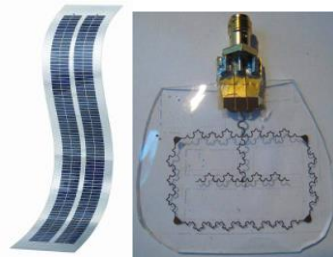
Figure 4.20. Circuits and antennas on a thin layer.

On a macro level, 'radio mirrors,' i.e., passive repeaters successfully used to transmit UHS signals in multisegment LOS to over 100 km, can be used to extend the range of environments that an ER can explore. **Figure 4.21** shows Microflect™ reflectors and how these were used in long-distance communication deployment). The use of multiple TFs enables the transmission of light or other electromagnetic signals around obstacles and/or into tunnels, further enabling exploration for the ER.

The reflective layer can be made to be very thin, of the order of microns.
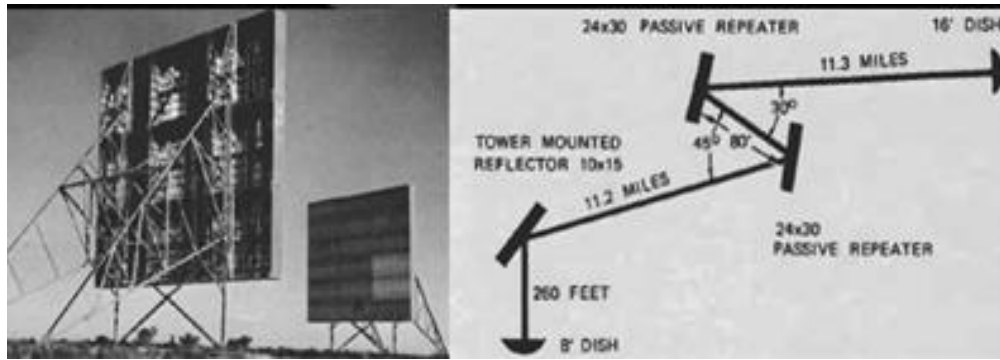
Figure 4.21. Reflection technology with large reflectors, terrestrial communications over 100 km.

Multifunction Integration

In some cases, it is possible to integrate all function in the same layer as illustrated in **Figure 4.22.** Stacking enables more efficient use of TF fabric where different layers performing sensing, computation, communication, and/or energy storage can occupy different vertical layers of the same horizontal space. In such a scenario, the only limitation is the allowable thickness of each layer. An alternative approach utilizes both the front and back of a thin structure, such as with the NASA ISARA cubesat. This project uses the bottom surface of a cubesat's solar arrays as a reflection antenna to boost signal bandwidth from kilobits to megabits.
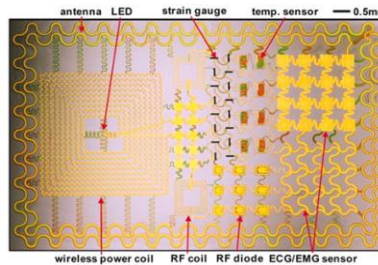
Figure 4.22. Multifunction integration in a thin layer of Epidermal electronics[19].

5 What's Done—What it Means, What's Next

5.1 Risks Revisited

Risk: No realistically designed TF is able to project enough solar energy to power a rover's operations (including providing adequate heating), for any representative mission.

Addressed: Optical analysis shows that exploration of large craters requires a 40-m diameter reflector, which is sufficient for a rover for each crater and cave scenario (more precisely the calculations show the size of a 40-m diameter is sufficient to provide needed solar energy for powering an MSL-class rover with $6m^2$ solar panel[8] at 10 km). Smaller craters and caves are compatible with 1- to 10-m diameter TFs. Thermal and control analyses show no significant constraints or show-stoppers. Trade-offs exist between the size of the reflector and solar panels.

Risk: TFs may have an adverse impact on explored environment, perturbing science integrity through lighting and heating of dark, cold sites.

Addressed: A literature review on the impact of incident sunlight on volatiles in lunar regolith suggests that the level of 300 W/m^2 would produce negligible effects if the duration of exposure is a few hours, due to high thermal inertia and low sublimation rate of ice. This may allow missions at the edge of the ice region, with the rover traveling back and forth to the ice area. Our Phase II proposal will include alternatives for minimizing the level of solar illumination on areas of interest.

Risk: Hardware required to enable multiple functions of TF cannot be integrated into a single system.

Partially Addressed: The design did not reach sufficient maturity to allow a detailed analysis of integration. Many technologies to be integrated are themselves in TRL 3. There is no perceived deterrent, especially if a very flexible substrate is not needed, as was initially believed.

Risk: The TF shape cannot be controlled with sufficient accuracy and precision to enable projecting solar energy onto the rover's solar panels with high certainty, for any representative mission.

Partially Addressed: A preliminary analysis did not indicate any difficulty in pointing and tracking. A full answer requires, however, a more specific design. The main issue may be with projecting to a larger area; the risk of missing the solar panels is small.

**Risk:** The cost of TF solution is too high, such that it does not end up being a cost-effective way to enable science or exploration in EE.

Addressed: Several scenarios show TFs to be a cost-effective alternative compared to a $45M MMRTG. A more exact cost calculation would require design specifics for a design point; Phase II work addresses such a specific design.

5.2 Contributions to Space Technologies

This effort contributes to multiple Technical Areas (TA) of the NASA Space Technology Roadmap [28]: a) *TA04, Robotics and Autonomous Systems*, because in all respects TFs are a new class of robots/autonomous systems, built in 2D, but reconfigurable to 3D shapes, with capabilities beyond the projections of the Roadmap; b) *TA12, Materials, Structures, Mechanical Systems and Manufacturing*, as it addresses innovative types of lightweight and multifunctional

---

[8] A $6m^2$ solar power design for MSL existed as secondary alternative for the mission.

structures; and c) *TA03, Space Power and Energy Storage*, as it proposes innovative ways to redirect solar energy into shadowed exploration sites.

5.3 Outreach

The plan of Phase I was to disseminate the concept and results broadly, through a dedicated website and conference publications. This was achieved via talks, interviews in the media, publications, engagement of students, and by initiating various collaborations.

- **Collaboration Engagement with MIT:** Prof. Jeff Hoffman, ex-astronaut, and a team of his students in the Satellite Engineering class who worked on a project developing a concept for resource extraction in Lunar Cold Traps. *We will collaborate with Prof. Hoffman on future research in exploration of planetary cold traps using the TransFormers concept.*

- **Collaboration Engagement with Texas A&M:** Prof. John Valasek and his grad student James Henrickson, who has *applied for a NASA Space Technology Research Fellowship on this topic, and will likely come to JPL this summer to work on this problem with us.*

- **Internships:** Nine intern students from local colleges in the Los Angeles area worked on this project at JPL, in two groups, from September to January, and from January to May.

- **Talk** by Adrian Stoica as IEEE guest lecturer for the IEEE Bonaventura Section.

- **PodCast:** NASA Lunar Science Institute PodCast: http://cosmoquest.org/blog/365daysofastronomy/2013/12/17/dec-17th-future-lunar-explorers-could-be-transformers/

- **KISS Study Workshop:** Caltech hosted a Keck Institute of Space Studies (KISS) Workshop on Adaptive Multi-functional Space Structures for Micro-climate Control, May 19–23, 2014. The workshop was led by Co-I Dr. Marco Quadrelli, Prof. Sergio Pellegrino (Caltech), and Dr. James Lyke (AFRL), and included participants from other JPL divisions, as well as several external participants. PI Adrian Stoica gave the opening talk on TransFormers for Extreme Environments, part of the morning short course titled, Multifunctional Energy Projecting Systems for Planetary Exploration. The course was open to the public.
  The scope of the study is to adapt the most recent advances in multifunctional reconfigurable and adaptive structures to enable a micro-environment control that enables space exploration in extreme environments. The primary benefit of this study was to enable missions that would otherwise be too technologically challenging and/or expensive, in particular those that would involve long periods of time without direct solar input or RTGs, the availability of which may be limited in the future.

Publications

- Paper submitted to ISAIRAS on the topic of "TransFormer Shape Optimization for Microenvironment Projection Using Computational Intelligence"
- Paper submitted to AIAA SPACE2014 on "Transformers for Extreme Environments"

5.4 This Study in Context

A 2003 NIAC Phase I study *Extraterrestrial Caves: Science, Habitat, and Resources* (Boston, PI) focuses on developing technology to adapt existing caves into specific habitats for humans. This study focuses on environmental control to allow autonomous rover ER systems to do planetary exploration.

The Phase II 2011 NIAC on *Cavehopping Exploration of Planetary Skylights and Tunnels* (Whittaker, PI) focuses on mobility solutions of ER. This study is complementary and focuses on energy redirection and coordination between different assets on the surface. Their resources come through a tether, which in long-distance exploration, will run into performance limitations.

The 2011 Phase I NIAC on *SPS-Alpha: Solar Power Satellite via Arbitrarily Large Phased Array* (Mankins, PI) focuses on a novel, biomimetic approach to the challenge of space solar power, making possible the construction of huge platforms from tens of thousands of small elements that can deliver remotely and affordably 10s to 1000s of megawatts using wireless power transmission to markets on Earth and missions in space. This study also deals with an application of directed energy, focused primarily on delivering power at a distance to distributed ground assets.

The 2011 Phase II NIAC on *Printable Spacecraft* (Short, PI) focuses on the concept of designing and fabricating a spacecraft based entirely on flexible substrate 2D printed electronics. This study extends this concept by considering multifunctional systems, which also include embedded actuation.

The 2012 Phase I NIAC on *Growth Adapted Tensegrity Structures* (Longman, PI) describes a novel approach to create and engineer an economically viable space habitat development technology, for deployment of a lightweight tensegrity habitat structure orbiting at Earth-Moon L2, where onboard robotic assets will use space-based materials to provide water for shielding, irrigation, and life support; provide soil for ecosystem development; and enable structural maintenance and enhancement. This study leverages the tensegrity paradigm as a modality of origami-based folding for deployable structures.

5.5 New Openings

The study confirms that TFs could create favorable micro-environments in EE, and brings a novel perspective that enables new classes of missions. The first step, with highest return on investment at present, is to think further in the context of a mission to the Moon, at Shackleton crater. However, the concept is still young, and a number of important questions remain to be answered, including how the TF would unfold, perhaps origami-style; how would it be built as a multifunctional structure; and how would it operate autonomously.

At this time, the evaluation of a specific design is needed, and based on this study, a good target could be a 1000-m^2 surface that folds within a fraction of 0.1 m^3 and weighs 10 kg; this would be an ambitious, yet possibly feasible target for a TF module, and an easily modular payload, scalable, even for a MER. The Lunar Flashlight solar sail to be used to reflect light from orbit into polar craters of the Moon, will pack 80 m^2 in a 6-U cubesat (~0.006 m^3). For the Shackleton TF, we target about 15 times the area, while the cubesat solution would unfold to 150 times the area from an equivalent 1 m^3, which seems to indicate that, at least from the packing and reflector functionality, the task is doable. Moreover, this suggests it may be feasible to pack the surface of 1200 m^2 within 0.1 m^3, hence the push for Phase II to explore such designs. These reflectors have low mass. A tensegrity-based analysis for the structural elements to support the reflective surface also indicates a mass below 100 kg; these will be included in recommendations for further study.

There are a number of characteristics of the lunar environment not addressed in this Phase I study that are of importance as they will assist in eliminating risks to a mission: reduced gravity (~ 1/6th of the gravity on Earth), radiation (cosmic rays, the solar wind, and solar flares), micrometeoroid bombardment (in the range from 10 g to 100 kg with velocities ranging from 2.4

to 72 km/s). The electrostatic charging of lunar dust reduces surface reflectivity, lowering the efficiency of the reflector, while also reducing the emissivity of the surface, thus lowering the radiative properties and may create thermal control problems. A robustness study should be performed to see how these elements impact TF design.

A solution to caves and alternatives to project a more focused beam to the rover limiting the spill to neighboring areas involves a multisegment path, beyond the line of sight of a single TF, thus needing a multi-hop/multi-reflection solution with multiple TFs; this needs further study and is proposed to be addressed in the follow-on study.

TFs have the potential to enable new *very different* classes of missions, including: low-cost missions with multiple rovers for large-scale exploration, mining, and construction of infrastructure, and powering of a lunar base and warming up the area around it. TFs could be the first step towards establishing a permanent presence on the Moon, since they would provide an energy infrastructure to power all developments in the area by NASA and its partners.

First, there is the potential to support multiple platforms at once, either all under one beam of sunlight in a common area, or in different areas by multiple beams or time-shared beams. This is especially critical for small platforms, which presently cannot be accomplished due to the mass/volume overhead of the power and thermal subsystems. Rovers can adventure many kilometers around areas of interest.

TFs can be deployed in staged missions, with assets to be powered coming in later launches. Most importantly, TFs can support a permanent presence, over multiple missions, i.e., providing for many types of assets that would save on power/thermal; these could come even decades apart.

5.6 Recommendations for Future Work

Advance the TF concept in the context of a mission scenario at Shackleton crater, with:

1. **Focus on a polar volatiles mission**—with a detailed mission concept analysis, eliminate highest remaining risks, increase TRL to 3, providing:
   - Robustness solutions to dust, radiation, and meteorites;
   - Option of multi-hop reflections to project beyond line of sight, **helping controlled energy focus to reduce spill—key for missions into caves/lava tubes;**
   - Design study targeting a scalable TF unit of 1000 m^2 with a 100-micron (0.1 m^3) layer and weight of 10 kg
2. Tap into the potential of new classes of missions
   - Simultaneous powering/warming of multiple robots for effective mining, construction, and large-scale exploration; large area projection for a lunar base
   - A permanent multi-mission resource in the polar area of value to NASA and its partners

6   Conclusion

6.1   Summary of the Work

In this report, we have documented the findings of the Phase I study entitled "TransFormers for Extreme Environments". We met the goals set forth in the proposal, and determined new opportunities, challenges, and risks for advancing the concept, which we propose to explore further in a Phase II study. We provided a general description of the TF concept and how it can assist in creating a favorable micro-environment within a hard-to-survive-in extreme environment, focusing on providing power and heat to rovers operating in cold, dark places on the Moon, Mars, and Mercury. We determined requirements for TFs from a high-level analysis of four mission scenarios, and a more refined analysis of the most promising one, the Lunar South Pole scenario—most promising from the point of view of applicability and timeliness. The benefits of a TF to these missions was assessed. We provided a brief evaluation of the state of the art in industry for the functional areas that make subsystems of a TF, from electronics to sensing and actuation, and explored novel modalities in unfolding a large surface. We identified the directions that are most relevant for advancing the concept.

6.2   Final Words

TransFormers introduce a new way of looking at missions in extreme environments with the idea that we can control only target local areas of interest, creating favorable micro-environments within extreme environments. This works very well for robotic explorers, providing a survivable region around it; it can be used in conjunction with conventional approaches to extreme environments, for extending the envelope of use, and for lowering costs. It also works very well for human exploration; in fact, while an unmanned vehicle could receive heat and power from a nuclear RTG source, this is not a good option for a surface vehicle carrying astronauts. Also, an entire region around a lunar base, at the surface or under the surface, can be 'climatized', receiving direct or indirect (through multiple reflections) sunlight, making the area habitable to humans/terrestrial life.

The TransFormers technology leverages advances in several areas. Solar power technologies are one—and here there is a whole spectrum, from solar panels, heliostats, concentrators, reflectors, and selective reflectors. In particular, driven by space applications, there is the field of deployable space solar technologies, which allow the deployment of compact stowed configurations to large surfaces, now on the orders of 100 m^2, but able to produce much larger surfaces if needed. One needs to find the trade-offs between one large surface and several smaller ones. The applications are not only for space—controlling micro-climates on Earth will increase largely as the cost of the technologies has reached values that make it ready for public and personal use. The use of large-size reflectors to light shaded valleys in the towns of Ryukan, Norway and Viganella, Italy, is just a start. Furthermore, solutions for individual households are now available, with $300 heliostats being sold for the purpose of directing sunlight through house windows facing north (in Northern Hemisphere).

TFs are a new class of shape-changing robotic systems. Folding in origami patterns, with 'bones' of tensegrity structures and 'skin' of multifunctional surfaces (indeed leveraging on 'electronic skins' and similar means of embedding systems in thin, flexible/stretchable surfaces), these shape-changing robots now designed for a simple function are prone to diversify their role, both on Earth and in space. For interplanetary

missions, the TFs now imagined for surface operations use could become starting designs for shape-changing spacecraft, or surface explorers that morph from long-legged, large, insect-like robots rapidly moving inside caves, to large, winged robotic insects that can fly.

While these scenarios are futuristic, the benefits of TFs as a means to control micro-environments are clear and present. TFs enable new classes of missions of high scientific and exploration value in the relative close proximity to Earth, at low costs, without RTGs. TFs also provide an avenue for missions with many rovers, less burdened by power and heat loads, with low cost since they were built to terrestrial grade components—they would operate in climatized landscapes—and with less concern of failure since they are multiples. This truly opens the door for cooperative robotic operations, from scientific exploration to exploitation of resources.

NASA-developed TFs at the Lunar South Pole, or wherever points of high interest emerge, will be able to serve the mission of all NASA partners. This will be the first asset of true benefit for many; designed for a sufficient lifetime and strategically located, it would start an essential infrastructure on the Moon, and serve as a model for later expansion to other places.

7 Bibliography

1. Slade, M. A., B. J. Butler, and D. O. Muhleman (1992), Mercury radar imaging: Evidence for polar ice, Science, 258, 635–640, doi:10.1126/science.258.5082.635.

2. Lawrence, D. J. et al. (2013) Evidence for Water Ice Near Mercury's North Pole from MESSENGER Neutron Spectrometer Measurements, Science 339 (6117), 292-296.

3. Paige, D. A. et al. (2013) Thermal Stability of Volatiles in the North Polar Region of Mercury, 339 (6117), 300-303.

4. Spudis, P. D., et al. (2010), Initial results for the north pole of the Moon from Mini-SAR, Chandrayaan-1 mission, Geophys. Res. Lett., 37, L06204, doi:10.1029/2009GL042259.

5. Cushing, G. E., T. N. Titus, J. J. Wynne, and P. R. Christensen (2007), THEMIS observes possible cave skylights on Mars, Geophys. Res. Lett., 34, L17201, doi:10.1029/2007GL030709.

6. G.E. Cushing – Candidate cave entrances on Mars. Journal of Cave and Karst Studies, v. 74, no. 1, p. 33–47. DOI: 10.4311/2010EX0167R.

7. Haruyama, J., et al. (2009), Possible lunar lava tube skylight observed by SELENE cameras, Geophys. Res. Lett., 36, L21206, doi:10.1029/2009GL040635.

8. Leveille, R. J. and Datta, S. (2010) Lava tubes and basaltic caves as astrobiological targets on Earth and Mars: A review, Planet. Space Sci., 58, 592-598.

9. IEEE J Photovoltaics 2012, V2, 35.

10. IEEE Trans. Electron Devices 2011, V58, 1433.

11. IEEE Conf MEMS 2001, 511.

12. Adv Manufacturing Tech 2007, V38, 463.

13. J. MEMS'97, 465.

14. IEEE Robotics& Aut. Mag, 2010, V17, 78   .

15. Science 2006, V314, 1754.

16. IEEE Trns Comp. & Packaging Tech. V33 p754 2010.

17. IEICE Trans on comms, 2007, E90-B(9), 2225.

18. Novel Technologies for Elastic Microsystems: Development, Characterization and Applications 2011, http://www.cmst.be/publi/docfb2.pdf

19. Epidermal Electronics (Science, ID: 1206157, 2011).

20. 3D-WLP: www.imec.be/ScientificReport/SR2008/HTML/1224991.html

21. Towards a Programmable Material, MIT, (2000), http://groups.csail.mit.edu/mac/projects/amorphous/Progmat/thesis/

22. An Origami-Inspired Approach to Worm Robots IEEE/ASME Trans on Mechatronics, Vol. 18, No. 2, April 2013

23. Eyeglass telescope http://www.langorigami.com/science/technology/eyeglass/eyeglass.php

24. Deployable Antenna http://www.faqs.org/patents/app/20120193498

25. [NASA_GC] NASA Space Technology Grand Challenges, http://www.nasa.gov/pdf/503466main_space_tech_grand_challenges_12_02_10.pdf

26. "Vision and Voyages for Planetary Science in the Decade 2013-2022", NRC Committee on the Planetary Science Decadal Survey Space Studies Board, 2011.

27. "NASA Technology Area 10 Roadmap: Nanotechnology", NRC Report November 2010.

28. "NASA Technology Area 04 Roadmap: Robotics, Tele-robotics and Autonomous Systems", NRC Report November 2010.

29. L. Del Castillo, A. Moussessian, R. MacPherson, T. Zhang, Z. Hou, R. Dean, R. Johnson, "Flexible Electronic Assemblies for Space Applications," IEEE A&E Systems Magazine, June 2010.

30. PARC, a Xerox Company, Capabilities Overview "Printed and Flexible Electronics Services: Application development".

31. Y. Bar-Cohen and Qiming Zhang, "Electroactive Polymer Actuators and Sensors," Special Issue dedicated to EAP, Materials Research Society (MRS) Bulletin Vol. 33, No. 3, (March 2008) pp. 173-177.

32. "Printable, Organic and Flexible Electronics Forecast, Players and Opportunities, 2012-2022", Market Analysis, Cambrdige, MA: IDTechEx, 2012, Raghu Das and Dr Peter Harrop.

33. "The Sun to the Earth and Beyond – a Decadal Research Strategy in Solar and Space Physics", NRC Committee on the Solar and Space Physics Space Studies Board, 2003.

34. "Origami That Folds Itself", *Nature on-line*,

35. "Solar and Space Physics: A Science for a Technological Society", NRC Committee on

36. Boston, P. J. (2011) Extraterrestrial caves: A Solar System wide prospectus. *In* 1st International Planetary Caves Workshop, Oct 25-28, 2011, Carlsbad, NM. Lunar & Planetary Institute, Houston TX. Abstract #8027.

37. W.T. Welford and Roland Winston, *The Optics of Nonimaging Concentrators: Light and Solar Energy*, Academic Press, 1978.

38. NASA Space Technology Roadmaps http://www.nasa.gov/offices/oct/home/roadmaps/

39. A. Jain, Robot and Multibody Dynamics: Analysis and Algorithms, ISBN 978-1-4419-72668-8

40. [Andreas] Edgar L Andreas: New estimates for the sublimation rate for ice on the Moon, U.S. Army Cold Regions Research and Engineering Laboratory, 72 Lyme Road, Hanover, NH 03755-1290, USA, Icarus, Volume 186, Issue 1, January 2007, Pages 24–30.

41. [Burke] Burke, J. D., Merits of A Lunar Polar Base Location, Lunar Bases and Space Activities of the 21st Century. Houston, TX, Lunar and Planetary Institute, edited by W. W. Mendell, 1985, p.77.

42. [Bryant] Bryant, S.: Lunar Pole Illumination and Communications Maps Computed from Goldstone Solar System Radar Elevation Data, in The Interplanetary Network Progress Report, Volume 42-176, 2009, Fabrizio Pollara, Editor in Chief, http://ipnpr.jpl.nasa.gov/progress_report/42-176/176C.pdf

43. Boston, P.J., Frederick, R.D., Welch, S.M., Werker, J., Meyer, T.R., Sprungman, B., Hildreth-Werker, V., Thompson, S.L., and Murphy, D.L., 2003, Human utilization of subsurface extraterrestrial environ- ments: Gravitational and Space Biology Bulletin, v. 16, no. 2,p. 121–131

44. Bernardi, Nicola Ferralis, Jin H. Wan, Rachelle Villalon and Jeffrey C. Grossman, Solar energy generation in three dimensions, Energy Enviro. Sci. , 2012,5, 6880 http://zeppola.mit.edu/pubs/APPLAB967071902_1.pdf

45.   Bombardelli, C., Lorenzini E.C., and Quadrelli, B.M.: *Dynamical Effects of Solar Radiation Pressure on a Spinning Tether System for Interferometry*, presented at the 14th AAS/AIAA Space Flight Mechanics Meeting, Maui, Hawaii, February 8-12 2004.

46.   [Bussey] Bussey, D. Ben J.; Lucey, Paul G.; Steutel, Donovan; Robinson, Mark S.; Spudis, Paul D.; Edwards, Kay D.: Permanent shadow in simple craters near the lunar poles, Geophysical Research Letters, Volume 30, Issue 6, pp. 11-1, CiteID 1278, DOI 10.1029/2002GL016180.

47.   [Brandhorst] Brandhorst, H., Rodiek, J. A., O'neill, M., Eskenazi, M.: Ultralight, compact, deployable, hi-performance solar concentrator array for lunar surface power, http://www.carbon-free-energy.com/papers/2006/lunar_solar_array.pdf

48.   D. W. Beaty, *et al.*, 2004, Planning for a Mars in situ sample preparation and distribution (SPAD) system: *Planetary and Space Science*, v. 52, p. 55-66.

49.   J.D. Carpenter, R. Fisackerly, D. De Rosa, B. Houdou . Scientific preparations for lunar exploration with the European Lunar Lander, Elsevier, Planetary and Space Science, Volume 74, Issue 1, December 2012, Pages 208–223

50.   De Rosa, Diego, et al. "Characterisation of potential landing sites for the European Space Agency's Lunar Lander project." Planetary and Space Science 74.1 (2012): 224-246.

51.   ESO - European Southern Observatory 40m European Extremely Large Telescope (E-ELT) telescope (http://www.eso.org/public/news/eso1225/)

52.   [Farabet2013] -- Farabet, C.; Couprie, C.; Najman, L. & LeCun, Y. Learning hierarchical features for scene labeling *Pattern Analysis and Machine Intelligence, IEEE Transactions on, IEEE,* 2013, *35*, 1915-1929

53.   [Hinton2006] -- Hinton, G. E.; Osindero, S. & Teh, Y.-W. A fast learning algorithm for deep belief nets *Neural Comput., MIT Press,* 2006, *18*, 1527-155

54.   Ingham, M., Day, J., Donahue, K., Kadesch, A., Kennedy, A., Khan, M., Post, E., and Standley, S., "Model-based Approach to Engineering Behavior of Complex Aerospace Systems", *AIAA Infotech@Aerospace Conference 2012*, Garden Grove, CA, June 2012.

55.   Ingham, M., Rasmussen, R., Bennett, M., and Moncada, A., "Engineering Complex Embedded Systems with State Analysis and the Mission Data System", *AIAA Journal of Aerospace Computing, Information and Communication*, Vol. 2, No. 12, 2005, pp. 507-536.

56.   Ingham, M.D. and Crawley, E.F., "Microdynamic Characterization of Modal Parameters for a Deployable Space Structure", *AIAA Journal*, Vol. 39, No. 2, 2001, pp. 331-338.

57.   [Koren] Y. Koren, J. Borenstein, "Potential Field Methods and Their Inherent Limitations for Mobile Robot Navigation," Proceedings of the 1991 IEEE International Conference on Robotics and Automation, Sacramento, California – April 1991.

58.   [Koo2012] -- Koo, M.; Park, K.-I.; Lee, S. H.; Suh, M.; Jeon, D. Y.; Choi, J. W.; Kang, K. & Lee, K. J. Bendable inorganic thin-film battery for fully flexible electronic systems *Nano letters, ACS Publications,* 2012, *12*, 4810-4816

59.   [Landis] Landis, G. A., Bailey, S. G., Brinker, D. J., Flood, D. J.: Photovoltaic power for a lunar base, Acta Astronautica, vol. 22, pp. 197-203, 1990. [Li1] Xiongyao Li, Wen Yu, Shijie Wang, Shijie Li, Hong Tang, Yang Li, Yongchun Zheng, Kang T. Tsang, Ziyuan Ouyang: Condition of Solar Radiation on the Moon, in Moon 2012, pp 347-365.

60.   [Li2] Li, Xiongyao; Wang, Shijie; Zheng, Yongchun; Cheng, Anyun: Estimation of solar illumination on the Moon: A theoretical model, Planetary and Space Science, Volume 56, Issue 7, p. 947-950.

61. [Li2012] -- Li, N.; Zheng, M.; Lu, H.; Hu, Z.; Shen, C.; Chang, X.; Ji, G.; Cao, J. & Shi, Y. High-rate lithium--sulfur batteries promoted by reduced graphene oxide coating *Chemical Communications, Royal Society of Chemistry,* 2012*, 48*, 4106-4108

62. [LunarSourceBook] Lunar SourceBook, http://www.lpi.usra.edu/publications/books/lunar_sourcebook/

63. [Mercury_Craters] http://en.wikipedia.org/wiki/List_of_craters_on_Mercury

64. Mettler E., Breckenridge W.G., and Quadrelli M.B., "Large Aperture Telescopes in Formation: Modeling, Metrology, and Control,," The Journal of the Astronautical Sciences, vol. 53, no.5 October-December 2005, pp. 391-412.

65. Mitchell, K. L. (2005) Coupled conduit flow and shape in explosive volcanic eruptions. *J. Volcanol. Geotherm. Res.*, doi:10.1016/j.jvolgeores.2004.09.017.

66. Oberbeck, V.R., Quaide, W.L., and Greeley, R., 1969, On the origin of Lunar sinuous rilles: Modern Geology, v. 1, p. 75–80

67. Pankine, A., L. K. Tamppari, M. D. Smith, 2010. MGS TES observations of the water vapor above the seasonal and perennial ice caps during northern spring and summer, *Icarus* 210, 58–71, doi:10.1016/j.icarus.2010.06.043.

68. [QuadrelliHerd] Quadrelli, B.M., Kowalchuck, S., and Chang, J.: *Dynamics and Control of a Herd of Sondes Guided by a Blimp on Titan*, presented at the 14th AAS/AIAA Space Flight Mechanics Meeting, Maui, Hawaii, February 8-12 2004.

69. [QuadrelliIEEE] Quadrelli M.B., Zimmermann, W., Chau, S.: *System Architecture for a Guided Herd of Robots for Surface/Sub-Surface Exploration of Titan*, presented at the 2004 IEEE Aerospace Conference, Big Sky, MT.

70. Quadrelli, B.M.,et al, "Investigation of Phase Transition-Based Tethered Systems for Small Body Sample Capture," Acta Astronautica, 68, (2011), 947-973.

71. Quadrelli, B.M., West, J., "Sensitivity Studies of the Deployment of a Square Solar Sail with Vanes," Acta Astronautica, vo. 65, October-November 2009, pp. 1007-1027.

72. Quadrelli M. and Lorenzini E.: *Dynamics and Stability of a Tethered Centrifuge in Low Earth Orbit*, The Journal of the Astronautical Sciences. Vol. 40, Issue 1, Jan.-March 1992.

73. [Ryu2014] -- Ryu, S.; Noh, J. H.; Jeon, N. J.; Kim, Y. C.; Yang, W. S.; Seo, J. W. & Seok, S. I. Voltage Output of Efficient Perovskite Solar Cells with high Open-Circuit Voltage and Fill Factor *Energy & Environmental Science, Royal Society of Chemistry,* 2014

74. [Reif] J. H. Reif, H. Wang, "Social Potential Fields: A Distributed Behavioral Control for Autonomous Robots," Robotics and Autonomous Systems 27 (1999) 171-194.

75. Seborg, D. E., T. F. Edgar, and D. A. Mellichamp. 1989. Process Dynamics and Control, John Wiley & Sons, NY.

76. Spencer, D. A., *et al.*, 2009. Phoenix Landing Site Selection and Hazard Assessment, *submitted to J. Spacecraft and Rockets.*

77. [Shackleton] http://www.lunarlandclaimsandregistry.com/shackleton-crater.html

78. Stoica, A.: Transformers – Shape changing Space Systems Built with Robotic Textiles, 2011 ReSpace/MAPLD (Revolutionary Electronics in Space) Conference, Albuquerque, NM, 2011

79. Tamppari, L. K., *et al.*, 2011. Effects of Extreme Cold and Aridity on Soils and Habitability: McMurdo Dry Valleys as an Analog for the Mars Phoenix Landing Site, *Antarctic Science*, doi:10.1017/S0954102011000800.

80. Tamppari, L. K., *et al.,* 2009. Phoenix and MRO Coordinated Atmospheric Measurements, 115, E00E17, doi:10.1029/2009JE003415, 2010

81. Tamppari, L. K., et al., 2008. The expected atmospheric characteristics during the Phoenix mission, *J. Geophys. Res.,* 113 (E00A20), doi:10.1029/2007JE003034.

82. Tamppari, L. K., *et al.*, 2008. Water-ice clouds and dust in the north polar region of Mars using MGS TES data, *Planetary and Space Sciences* 56, 227-245.

83. [Tompkins] Paul Tompkins and Ashley Stroupe: Icebreaker: An Exploration of the Lunar South Pole, Proceedings of the 14th SSI Conference on Space Manufacturing, May, 1999.

84. [Veelaert] P. Veelaert and W. Bogaerts, "Ultrasonic Potential Field Sensor for Obstacle Avoidance," IEEE Transaction on Robotics and Automation, Vol. 15, No. 4, August 1999.

85. [Yang2014] -- Flexible Three-Dimensional Nanoporous Metal-Based Energy Devices Yang Yang, Gedeng Ruan, Changsheng Xiang, Gunuk Wang, and James M. Tour *Journal of the American Chemical Society* 2014 *136* (17), 6187-6190

86. Whiteway, J. A., *et al.,* 2009. Mars water ice clouds and precipitation, *Science,* 325 (5936), pp. 68-70.

87. [Wellford] W.T. Welford and Roland Winston, *The Optics of Nonimaging Concentrators: Light and Solar Energy*, Academic Press, 1978.

8   Acknowledgement of Support

Many thanks to all who made this study possible, and who are acknowledged in the following.

Experts:

- The JPL Team-A performed two Team-A sessions and considerable off-line work in between. This includes the following JPL domain experts: John Elliott, Gary Gutt, Daniel Klein, Jeff Nosanov, John Ziemer, Michael Johnson, and Kelli McCoy. A considerable part of this effort was the work of Gary Gutt who did the optical analysis and Daniel Klein who did the thermal analysis.
- Yosi Bar-Cohen and Mircea Badescu contributed to understanding deployment options and actuation alternatives.
- Bob Skelton, UCSD, provided insight on tensegrity and origami, and calculations of mass for desired mechanical properties of a structure packed in 1 m^3.

Students, who had an important contribution in the experimental research:

- Eddie Lopez did a number of drawings that capture the concept, including the pictures on the cover of this report, and assembled heliostats and put them in operation.
- Anubhav Thakur, graduate student at USC, did physical modeling and simulation for origami-type deployments.
- Bahador Behdad and Renato Valtz-Brenta researched fabrication alternatives for TFs and means to deploy TFs; built a 60 cm × 60 cm Miura-ori deployable origami TF, actuated with telescopic car antennas; and also experimented with various shape-memory alloys for actuation. They also performed experiments with multireflection solutions and mirrors to power small solar rovers.
- Emma Kohany and Sam Shin experimented with mirrors and a heliostat that powered a Sojourner-scale rover at a few tens of meters.
- Greg Capra, Javier Sanchez, and Ali Jafari Ashtiani contributed to cellular computational models for distributed control of TF fabric.

Other collaborators:

Thanks to Schuyler Eldridge, PhD student at the University of Boston, who has a NASA Space Technology Research Fellowship. He contributed to the study of the implementation of TFs in thin, flexible technologies, and contributed to the final report.

Many thanks to Samantha Ozyildirim of JPL, who did an incredible job in bringing this report to correct expression and proper form—we are greatly indebted.

Thanks to JPL management for their suggestions during the review and for their support during this study.

We acknowledge Caltech's Keck Institute of Space Studies (KISS) for sponsoring and organizing a KISS workshop at Caltech during May 19–23, 2014. In particular, we thank Michelle Judd, the Managing Director. The workshop attracted over 25 experts in the field of multifunctional adaptive structures for solar energy projection, and was an excellent forum for looking ahead at concepts in this area, allowed a peer validation of the concepts, and triggered new avenues (selective reflection, 3D reflectors, tensegrity implementations) suggested for further study in the Phase II proposal.